

FRACTURE TOUGHNESS OF FABRIC REINFORCED EPOXY COMPOSITES USING J-INTEGRAL APPROACH

By

S. K. KHANNA

ME
1984

TH
ME/1984/14
K 527 f

M
KHA

FRA



DEPARTMENT OF MECHANICAL ENGINEERING
INDIAN INSTITUTE OF TECHNOLOGY, KANPUR
NOVEMBER, 1984

FRACTURE TOUGHNESS OF FABRIC REINFORCED EPOXY COMPOSITES USING J-INTEGRAL APPROACH

**A Thesis Submitted
In Partial Fulfilment of the Requirements
for the Degree of
MASTER OF TECHNOLOGY**

**By
S. K. KHANNA**

**to the
DEPARTMENT OF MECHANICAL ENGINEERING
INDIAN INSTITUTE OF TECHNOLOGY, KANPUR
NOVEMBER, 1984**

ME-1984-M-KMA-FRA

CENTRAL

87489

19 JUN 1985

23/11/84.
B2CERTIFICATE

This is to certify that the thesis entitled
" Fracture Toughness of Fabric Reinforced Epoxy Composites
Using J-Integral Approach" by S.K. KHANNA is a record of
work carried out under our supervision and has not been
submitted elsewhere for a degree.

B.D. Agarwal
Professor
Dept. of Mechanical Engg.
Indian Institute of Tech.
Kanpur-208016
India

Prashant Kumar
Assistant Professor
Dept. of Mechanical Engg.
Indian Institute of Tech.
Kanpur-208016
India

POST GRADUATE OFFICE
This thesis is approved for the award of degree of Master of Technology (Tech.) to the candidate Name of the candidate Institute of Technology, Kanpur Date: 29/12/84. B2

ACKNOWLEDGEMENT

I express my deep sense of gratitude and appreciation to Professors B. D. Agarwal and Prashant Kumar for their valuable guidance throughout the present work.

I am thankful to Mr. B.K. Mishra for the help rendered throughout the experimental investigation and in preparation of the manuscript.

Thanks are due to my colleagues Messers K. Srinivasan, K.K. Bajpai, R.K. Gupta who helped me during various stages.

Special thanks are due to Mr. B.K. Jain of Advanced Centre of Materials Science and Mr. S.N. Dwivedy of Experimental Stress Analysis Laboratory for the cooperation and help rendered throughout the experimental investigations.

Thanks are due to Messers S.L. Srivastava, D.K. Sarkar, Swaran Singh, R.S. Shukla and D.P. Saini of Mechanical Engineering Department for their help.

Last but not the least thanks are due to Mr. D.P. Saini for the excellent typing of the manuscript.

S.K. KHANNA

TABLE OF CONTENTS

	Page
List of Figures	iv
Nomenclature	viii
Abstract	ix
CHAPTER I	INTRODUCTION
	1
1:1 :	Introduction
	1
1:2 :	Fracture Mechanics of Composites
	2
1:3 :	Basis for J-Integral
	6
1:4 :	Scope of the Present Work
	16
CHAPTER II	EXPERIMENTAL DETAILS
	17
2:1 :	Material and Specimen Preparation
	17
2:2 :	Testing System
	21
CHAPTER III	EXPERIMENTAL RESULTS AND DISCUSSION
	23
3:1 :	0°/90° Plain Woven Cloth Laminates
	23
3:1.1:	Experimental Evaluation of J_{1C}
	27
3:1.2:	Effect of Specimen Length
	40
3:1.3:	Effect of Specimen Width
	58
3:1.4:	Effect of Style of Reinforcement on Mechanical Properties and Fracture Toughness
	67
3:2 :	Evaluation of J_{1C} for $\pm 45^\circ$ Laminates
	71
3:3 :	Conclusions
	76
3:4 :	Scope for Further Work
	77
REFERENCES :	78

LIST OF FIGURES

<u>FIGURE NO.</u>	<u>TITLE</u>	<u>Page</u>
1.1	Crack tip coordinate system and arbitrary line integral contour	7
1.2	A cracked body with constant (a) load applied (b) displacement applied	11
1.3	Generalized load deflection diagram with prescribed load	12
1.4	Generalized load deflection diagram with prescribed displacement	13
2.1	Experimental arrangement for cutting notches	20
2.2	Experimental arrangement on MTS machine	22
3.1	Stress-strain curve for laminates with type-A reinforcement	24
3.2	Stress-strain curve for laminates with type-B reinforcement	25
3.3	A SEN specimen showing J-integral contour	28
3.4	Load displacement curves for 100 mm long specimens with type-A reinforcement	29
3.5	Load displacement curves for 100 mm long specimens with type-B reinforcement	30

3.6	Variation of critical displacement with crack length for type-A reinforcement	32
3.7	Variation of critical displacement with crack length for type-B reinforcement	33
3.8	Strain energy per unit thickness for different displacements for 100 mm long specimens with type-A reinforcement	35
3.9	Strain energy per unit thickness for different displacements for 100 mm long specimens with type-B reinforcement	36
3.10a	J-integral curve for 100 mm. long specimens with type-A reinforcement for $a_0/w > 0.5$	37
3.10b	J-integral curve for 100 mm. long specimens with type-A reinforcement for $a_0/w < 0.5$	38
3.11a	J-integral curve for 100 mm. long specimens with type-B reinforcement for $a_0/w > 0.5$	39
3.11b	J-integral curve for 100 mm. long specimens with type-B reinforcement for $a_0/w < 0.5$	40
3.12	Load displacement curves for 75 mm. long specimens for type-A reinforcement	43
3.13	Load displacement curves for 150 mm. long specimens for type-A reinforcement	44

3.14	Load displacement curves for 75 mm. long specimens with type-B reinforcement	45
3.15	Load-displacement curves for 150 mm. long specimens with type-B reinforcement	46
3.16	Variation of critical displacement with specimen length for different initial crack length for type-A reinforcement	47
3.17	Specimen length vs. critical displacement for different initial crack length for type-B reinforcement	48
3.18	Variation of fracture strain energy with specimen length for different initial crack lengths for specimens with Type-A rein- forcement.	50
3.19	Variation of fracture strain energy with specimen length for different initial crack lengths for specimens with Type-B reinforcement	51
3.20	J-integral curves for specimens of different lengths for Type-A reinforcement	53
3.21	J-integral curves for specimens of different lengths for Type-B reinforcement	54
3.22	Influence of specimen length on J_C for type-A reinforcement	55

3.23	Influence of specimen length on J_C for Type-B reinforcement	56
3.24	Transmitted light photograph of two specimens with Type-A reinforcement, for different crack lengths	58
3.25	Strain energy at crack tip for different crack lengths	59
3.26	Load-displacement curves for 15 mm wide specimens	61
3.27	Load-displacement curves for 25 mm wide specimens	62
3.28	Load-displacement curves for 35 mm wide specimens	63
3.29	Load-displacement curves for 40 mm wide specimens	64
3.30	Effect of specimen width on critical displacements	65
3.31	J-integral curves for specimen of different width	67
3.32	Influence of width on J_C	68
3.33	Load-displacement curves for $\pm 45^\circ$ angle ply specimens	71
3.34	Variation of critical displacement with crack length for $\pm 45^\circ$ angle ply specimen	72
3.35	Strain energy per unit thickness for different displacements for $\pm 45^\circ$ angle ply specimens	74
3.36	J-integral curve for $\pm 45^\circ$ angle ply specimens	75

NOMENCLATURE

A	Area
a, a_0	Crack length , Initial crack length
d	Generalised displacement
F	Generalised force
G	Energy release rate
J	J-integral
J_{1C}	Critical value of J-integral in mode I
LEFM	L linear Elastic Fracture Mechanics
l	Length of the specimen
P	Load
r	Near tip crack field parameter
S	Boundary of a two dimensional body
S_T	Portion of boundary where traction is prescribed
SEN	Single edge notched specimen
T_i	Traction vector
t	Thickness
U	Potential energy per unit thickness
u_i	Displacement vector
v_f	Fiber volume fraction
W	Strain energy density function
w	Width
x_1, x_2	Co-ordinates
σ	Stress along load direction
σ_{ij}	Stress tensor
ϵ	Strain along load direction
Γ	J-integral contour
ν	Poisson's ratio

ABSTRACT

Fracture toughness of glass fabric reinforced epoxy resin has been investigated experimentally. Fracture tests were conducted on single edge notched specimens and J-integral evaluated using energy rate interpretation.

Laminates with two different styles of glass fabric reinforcement were tested, keeping volume fraction the same. In both cases the critical value of J-integral, J_{1C} , is found to be independent of crack length and specimen length when $a_0/w > 0.5$. For smaller crack lengths an extrapolation method has been used to separate the crack tip energy from the energy absorbed due to general material damage away from the crack-tip. The J-integral thus obtained is independent of crack length and specimen length, and is close to J_{1C} obtained for $a_0/w > 0.5$ without extrapolation. Laminates with fine, plain weave, balanced, singles yarn glass fabric reinforcement possess a higher fracture toughness than laminates with coarse, plain weave, balanced, plied-yarn glass fabric reinforcement. The type of twist

and plying of glass fibers significantly affects the fracture toughness. J_{1C} is also found to be independent of width for $a_o/w > 0.5$.

J_{1C} is found to depend strongly on fiber orientation. For $\pm 45^\circ$ laminates, J_{1C} is found to be very low.

CHAPTER-1

INTRODUCTION

1.1 INTRODUCTION:

Upto about two decades ago the main structural materials used were metals like iron, steel, aluminium etc. As the requirements on materials grew and became more stringent, different strength improving and toughness improving processes were developed. With the advent of the space age metals were not found suitable for all purposes. Then a new class of materials - composite materials, began to develop rapidly. Composite materials in some form or the other have existed for many years but fiber reinforced composite materials have developed extensively only in the last two decades.

A composite is a combined material created by the synthetic assembly of two or more components - a selected filler or reinforcing agent and a compatible matrix binder (e.g., a resin) - in order to obtain specific characteristics and properties. The main advantage of composites is that they can be designed to provide an almost unlimited selection of characteristics. Composite properties like light weight,

high specific strength, high stiffness, toughness, fatigue and corrosion resistance and high temperature performance have made them useful in practically all industries.

1.2 FRACTURE MECHANICS OF COMPOSITES:

Like all man made materials, composites also may contain defects and are susceptible to weakening due to development of cracks. Hence if composites are to be used as engineering materials, it is essential to develop material selection criteria and design procedures. To achieve this we must be able to predict the behaviour of composites in the presence of crack like defects. To this end fracture mechanics has been developed and widely accepted for metals.

Fracture mechanics is concerned with the study of fracture of materials by crack initiation and propagation. Fracture mechanics approach has been found useful in predicting the strength of homogeneous isotropic materials in the presence of flaws or cracks. It also provides guidelines for quality control and inspection requirements of components. Fracture studies of composite materials are more complicated because the self similar crack growth observed in homogeneous materials usually does not occur in composite materials.

In composites fracture may initiate due to any one or a combination of the following mechanisms: breaking of fibers, fiber pullout, debonding between fiber and matrix, fracture of the matrix etc. The crack growth in composites differs substantially from the cracks in traditional materials. The cracks are greatly dispersed forming a damage zone instead of a well defined crack surface. These complexities in composites underscore the need for combined experimental and theoretical analysis. Fracture mechanics of composites together with its initiation, propagation and controlling parameters represents a significant problem.

Since the advent of fracture mechanics, two basic approaches have emerged, namely, the energy approach and the stress approach. The first approach is due to Griffith [1] who on the basis of thermodynamic considerations derived a criterion for fracture, by taking account of the total energy change in a cracked body. The second approach is due to Irwin [2] who relied on stress analysis of a cracked body. According to him, the behaviour of a crack could be fully characterised through elastic stress intensity factor, K and it is equivalent to the Griffith's energy release rate, G . Irwin carried out stress analysis of cracked bodies assuming the material to be linear elastic. The approach

which assumes the material to be linear elastic is known as linear elastic fracture mechanics (LEFM).

LEFM concepts have also been applied to composite materials [3-7]. When a load is applied to a laminate with a crack, a region of subcritical damage appears and grows around the crack tip. If the dimension of this region at final failure is small enough

to affect the linear elasticity of gross behaviour, it seems plausible to expect the concepts of LEFM to apply. Still the problem is not solved and reduces to the following questions : (1) What are the variables that can describe the state of this tip region? (2) What are the critical values of these variables that dictate ultimate failure? The most difficult situation arises when diffused subcritical damage develops before final failure. LEFM cannot be expected to predict the final failure load. Moreover the problem is no longer two dimensional because delamination is involved. Failure at the crack tip cannot be described by a smooth fracture surface. In such a case we are not dealing with a 'crack extension'. The growth of subcritical damage until failure must be described. So researchers have proposed a new two parameter LEFM model, in place of the usual one parameter model, with the length of the damage zone as the second parameter.

There is a continuing search for a parameter to characterise fracture behaviour of a composite material which is independent of test variables. Various other methods have been developed to obtain fracture toughness, namely, the R-curve approach and the J-integral approach. The R-curve approach has been studied widely for metallic materials and has also been extended to composite materials [8-11]. Researchers have considered the damage zone as a self similar crack extension. The instantaneous crack length is estimated by a compliance matching procedure. This approach is somewhat lengthy and time consuming.

The J-integral approach proposed by Rice [12] characterises the crack tip area by a parameter without focussing attention directly at the crack tip. This is thus a more practical and easier method for analysing fracture. A two-dimensional energy line integral termed as J-integral is such a parameter. The use of the J-integral as an elastic-plastic fracture criterion has been discussed by Broberg [13] from an analytical standpoint. The basis for J-integral is provided by the works of Hutchinson [14] and Rice and Rosengren [15]. They have shown that a singularity in stress and strain does exist at the crack tip which is uniquely dependent upon the material flow properties. Mc Clintock [16] has

demonstrated that the crack tip stress and strain field can be described in terms of the J-integral. However, the independent nature of the integral allows an integration path taken sufficiently far from the crack tip to be substituted for a path close to the crack tip region. Begley and Landes [17] through extensive experiments have shown the applicability of J-integral as a fracture criterion for metals. Agarwal, Kumar and Patro [18] have applied J-integral as a fracture criterion for short glass fiber composites. They have demonstrated that the critical value of J-integral is independent of crack length. Srinivasan [19] has applied J-integral as a fracture criterion for oriented fiber composites. Smith, Green and Bowyer [20] attempted to apply J-integral approach to glass fabric reinforced polyester resins.

1.3 BASIS FOR J-INTEGRAL:

The J-integral as proposed by Rice [12], is a two dimensional energy line integral

$$J = \int_{\Gamma} (W dx_2 - T_i \frac{\partial u_i}{\partial x_1} ds) \quad (1.1)$$

where Γ is any contour traversing in a counter clockwise sense and enclosing the crack tip as shown in

Fig. 1.1. The components of traction vector are

$T_i = \sigma_{ij} n_j$ where σ_{ij} is the stress tensor and n_j a

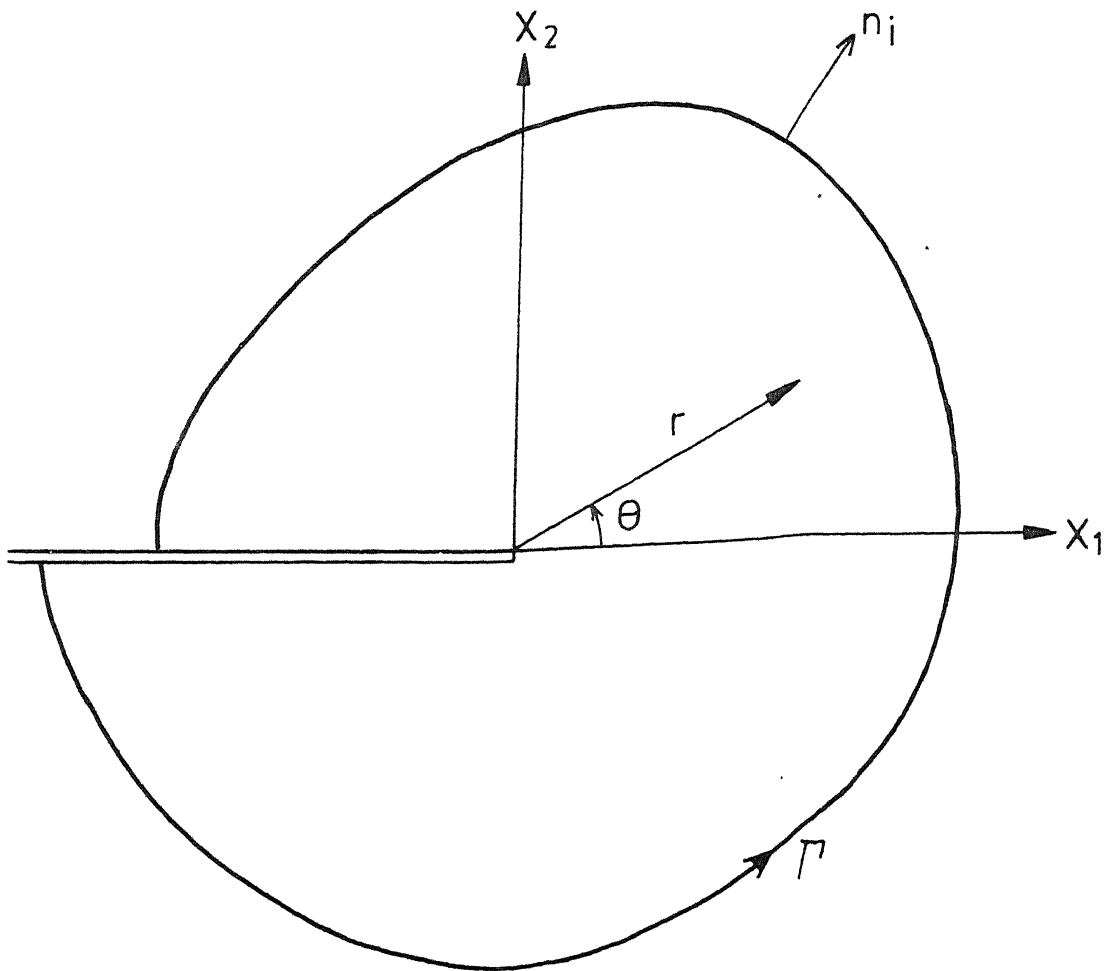


Fig. 1.1 Crack tip coordinate system and arbitrary line integral contour.

unit vector normal to Γ ; u_i is the displacement vector and s the arc length along Γ . W , the strain energy density, is defined as

$$W = W(\epsilon_{mn}) = \int_0^{\epsilon_{mn}} \sigma_{ij} d\epsilon_{ij} \quad (1.2)$$

where ϵ_{ij} is the strain tensor.

The J-integral characterizes the crack tip field, the basis of which is provided by the works of Hutchinson [14] and Rice and Rosengren [15]. They have extended fracture mechanics concepts to cases of large scale yielding which also assumes the existence of a crack tip singularity. They indicate that the product of plastic stress and strain approaches a $1/r$ singularity; r being a near tip crack field length parameter. The crack tip singularity is uniquely dependent on the material constitutive relations. For a deformation theory of plasticity, Mc Clintock [16] has demonstrated, through the crack tip plastic stress and strain equations expressed from the Hutchinson Rice Rosengren (HRR) singularity, the existence of a singularity in r whose strength is J-integral.

The J-integral has another important advantage as a fracture criterion. Broberg [13] considered crack growth criteria for a nonlinear elastic body containing

a crack. For such a body, stress and strain singularities occur at the crack tip. This region ahead of the crack tip is termed as the end region outside which the material may be regarded as a continuum. As the load is increased, the end region eventually reaches a critical state at which the crack starts moving. One prominent feature of the end region at critical state is that the state is neither dependent on the distribution of loads nor on the crack length. It simply and solely depends on the material itself. The end region can be specified by J-integral. Also, J-integral reaches a critical value, J_c , as the end region reaches the critical state.

From the foregoing discussion, it is evident that J-integral displays three prominent features attractive to its use as a fracture criterion namely,

- (i) J-integral as a field parameter indicates the stress and strain distribution in a cracked body.
- (ii) It describes the crack tip region by specifying the strength of the singularity.
- (iii) Critical value of J-integral, J_c is a material property which can be used as a fracture criterion when unstable crack growth occurs.

The J-integral can be conveniently evaluated experimentally through its energy rate interpretation.

It may be noted that in Eq. 1.1 the two terms in the integrand namely W and $T_i \frac{\partial u_i}{\partial x_1}$, have the dimensions of energy. Thus, J is a energy related quantity. In fact Rice [12] has shown that the J -integral is equal to the change in potential energy for a virtual crack extension

$$J = - \frac{\partial U}{\partial a} \quad (1.3)$$

where U is the potential energy per unit thickness. For a two dimensional elastic body of area A , with a boundary s , the potential energy is given by

$$U = \int_A W \, dx_1 \, dx_2 - \int_{S_T} T_i u_i \, ds \quad (1.4)$$

where S_T is the portion of the boundary over which traction, T_i is prescribed. A cracked body with prescribed boundary conditions is shown in Fig. 1.2. If the boundary conditions are given in terms of the generalised force, F , the potential energy is represented by the shaded area above the load displacement curve in Fig. 1.3a. In this instance the potential energy is negative and its magnitude is equal to the complementary energy [17]. When the boundary conditions are prescribed in terms of generalised displacements the second term in Eq. 1.4 drops out, since the traction \bar{T} on it is zero most of the time. The potential energy is then equal to the strain energy or the area under load deflection curve in Fig. 1.4a.

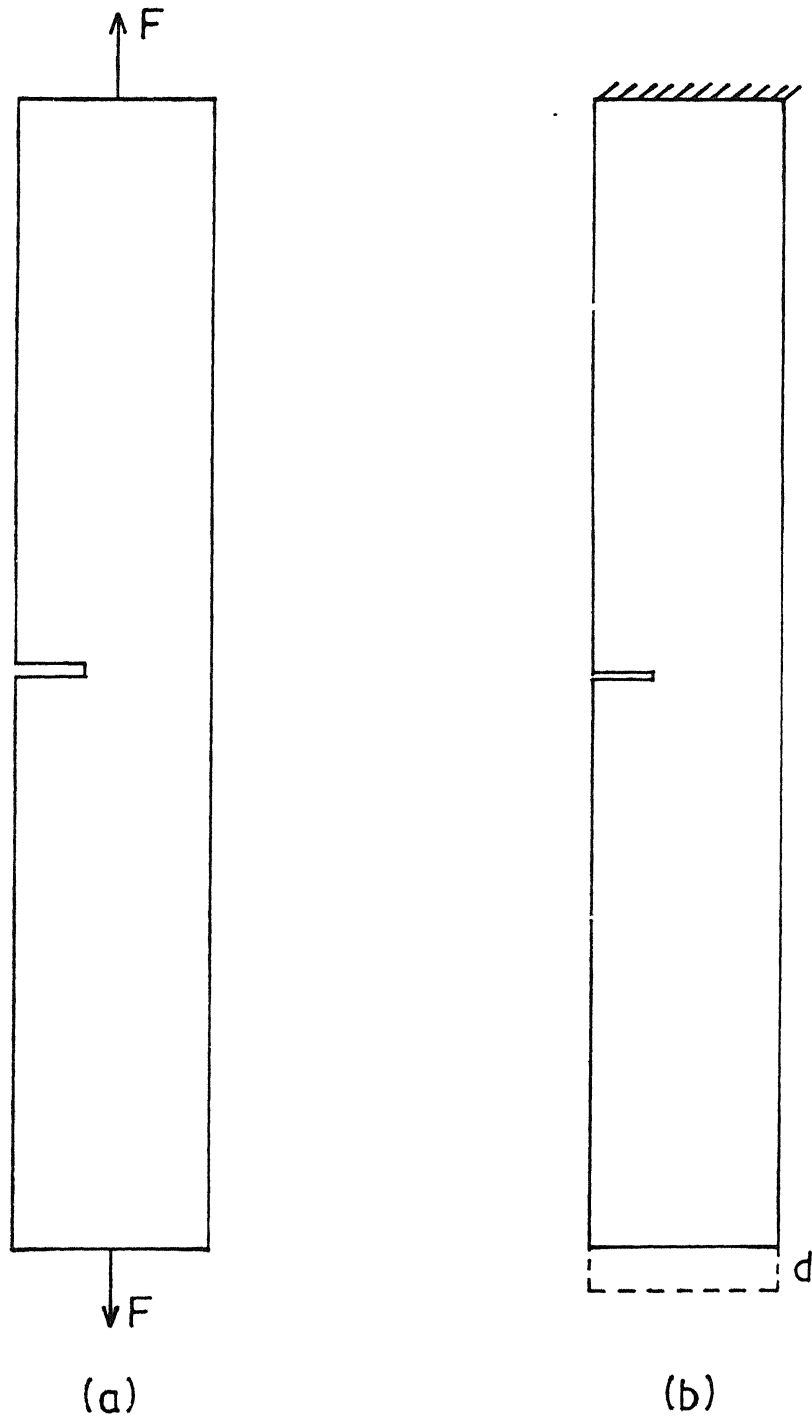


Fig. 1.2 A cracked body with constant
(a) load applied
(b) displacement applied

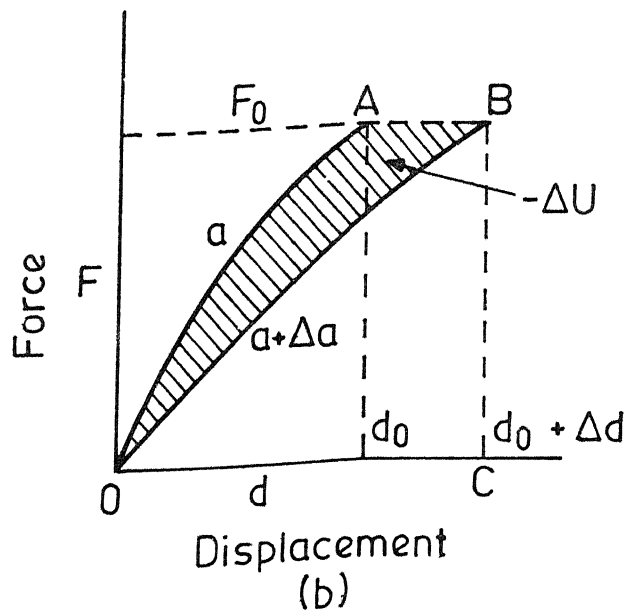
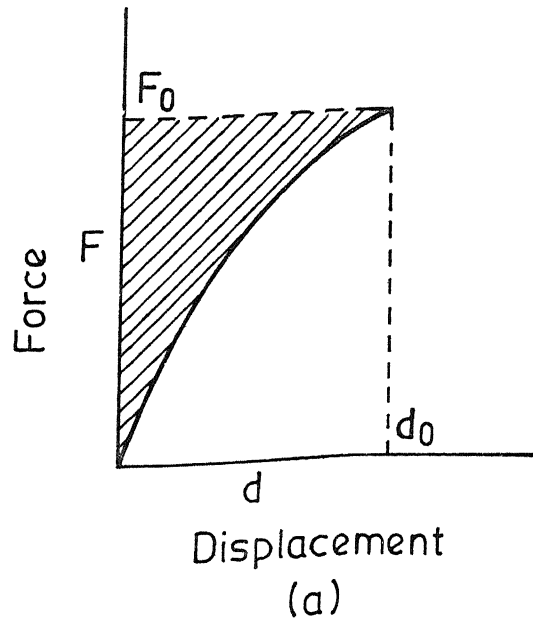


Fig. 1.3 Generalized load deflection diagram with prescribed load.

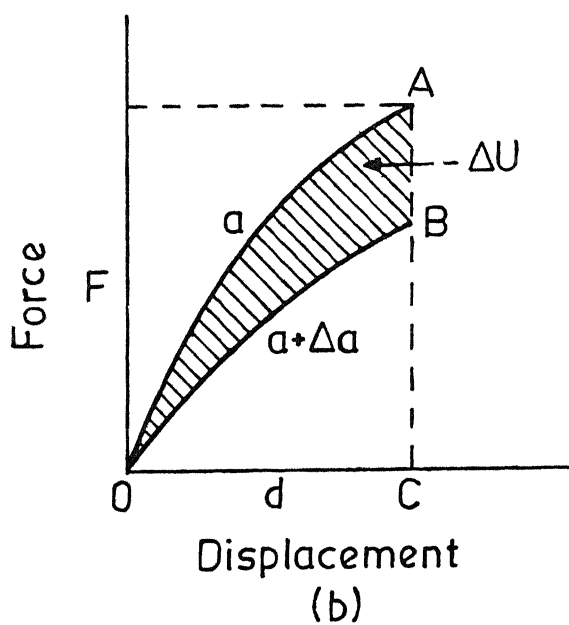
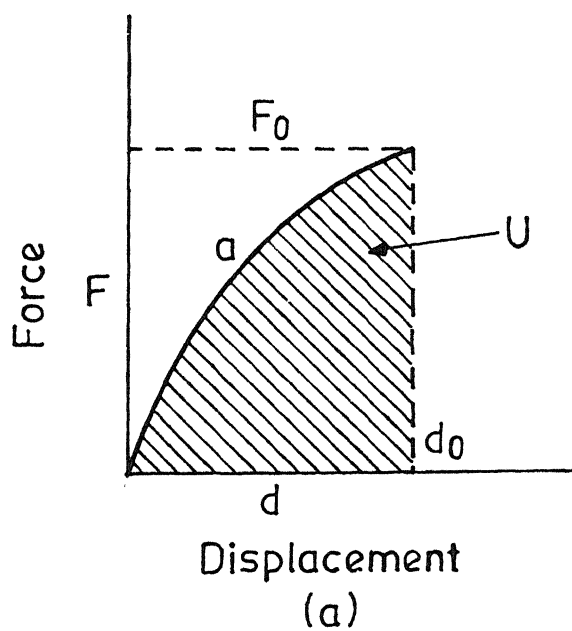


Fig. 1.4 Generalized load deflection diagram with prescribed displacement.

The J-integral can be evaluated considering the load deflection diagrams of similar bodies with neighbouring crack sizes. When two similar bodies with crack lengths a and $a + \Delta a$, are loaded, the load deflection curves are represented by OA and OB. If in the first body, the crack extends from a to $a + \Delta a$ under prescribed load, F_0 , the total work done on the body is represented by the area OABCO (Fig. 1.3b). Because of reversibility, the unloading curve from the point B is the same as the loading curve of the body starting with a crack length, $a + \Delta a$. The strain energy of the body with a crack length, $a + \Delta a$, under the load F_0 is the area OBCO. The shaded area OABO ($= \Delta U$) is the energy available for crack extension. Similarly when the crack extends from a to $a + \Delta a$, under prescribed displacements, the energy available for crack extension is the shaded area OABO (Fig. 1.4b). It may be mentioned that the difference in energy obtained by the two methods is of the second order. However, for an experimental evaluation of J-integral, the prescribed displacement boundary condition is preferable since, for two specimens of neighbouring crack sizes, the displacements at fracture are observed to be nearly equal, whereas the fracture loads are found to be quite different. Furthermore, for higher crack length specimens, at which J-integral is evaluated, the load-deflection

diagrams become flat and it is more appropriate to evaluate J in terms of displacement. In such a case, Eq. 1.3 can be written as

$$J = - \frac{\partial U}{\partial a} \quad \text{constant displacement} \quad (1.5)$$

Begley and Landes [17] have used the above relation to evaluate J -integral as a fracture criterion for metals. They demonstrated the applicability of J -integral for the case of large scale yielding at the crack tip through experimental results on an intermediate strength rotor steel. They observed that the J -integral at failure for fully plastic behaviour was equal to the linear elastic value of strain energy release rate (G) at failure for extremely large size specimens. Thus, the J -integral approach eliminates the necessity of testing very large specimens.

A major limitation of the approach arises from the fact that the J -integral is path independent only when the stress-strain relation is unique. It is truly path independent for linear and nonlinear elastic stress strain laws and also for elastic-plastic behaviour under situations of monotonic loading. This rules out its application to materials which exhibit significant sub-critical crack growth prior to fracture since any crack extension implies unloading near the crack tip.

1.4 SCOPE OF THE PRESENT WORK:

The present work attempts to characterise the fracture behaviour of glass fabric reinforced epoxy resin. Glass fabric is used for applications that require quick thickness build up over large areas. This characteristic is especially useful in the manufacture of fiberglass boats, various marine products, and some types of tooling. Glass fabric, many times coupled with graphite fabric, is used widely for making components in aerospace industry. Fabric reinforced composites have been found to be easy to fabricate and very effective in use. Hence because of the increasing use of glass fabric reinforced epoxy composites, they have been chosen for study of their fracture behaviour.

Details concerning material and specimen preparation and fracture toughness testing system are given in Chapter II. In Chapter III, the effect of crack length and specimen length on critical value of J-integral, for two different styles of glass fabric reinforcement, are reported. The effect of width on J critical is also investigated. Then the effect of ply orientation on J critical is investigated. $\pm 45^\circ$ plain weave glass fabric laminates have been tested.

CHAPTER-2

EXPERIMENTAL DETAILS

2.1 MATERIAL AND SPECIMEN PREPARATION:

The present studies were performed on glass fabric reinforced epoxy resin. Composite plates were fabricated using two different types of glass fabric reinforcement. Type A reinforcement used was fine, plain weave, balanced, singles-yarn (untwisted) glass fabric of the following specification:

Thickness : 0.12 mm
Weight : 144 g/m²
Count/in : 28 x 28 E-GLASS

Type B reinforcement used was coarse, plain weave, balanced, but of lower count or a more open weave pattern compared to A, plied-yarn (twisted) glass fabric of the following specifications:

Thickness : 0.32 mm
Weight : 272 g/m²
Count/in : 18 x 18 E-GLASS

The matrix material used was Araldite CY230 epoxy cured with 10% by weight of hardener HY951, both supplied by Ciba-Geigy of India, Ltd.

Composite plates were cast between two 25 mm thick mild steel mould plates, lined with mylar sheets and separated by mild steel washers to control thickness of the cast plate. Outer surface of each mould plate was heated through several insulated heating elements of 250 watts each which provided a uniform temperature distribution over the whole plate. The heating of the mould plates could be controlled through a transformer. The temperature of the plate during curing was measured with a copper-constantan thermocouple; one end of which was embedded in the composite plate and the other ends fixed to a digital milli-voltmeter.

Glass cloth pieces were cut to the required size and placed on the lower mould plate one by one. A small amount of resin was spread on the lower mould plate and on the top of each glass cloth piece. The resin was spread on the cloth piece by a rubber roller to enhance impregnation and to squeeze out any air bubbles. The composite plates were cured at a temperature of 55°C for 26 hours for improved properties over room temperature cure.

The fiber volume fraction obtained for type A reinforcement was 39.5% and the plate thickness was 2 mm. For type B reinforcement the obtained fiber volume fraction was 37.5% and plate thickness 3.5 mm.

Rectangular specimens were cut by a diamond impregnated wheel, cooled by running water. All fracture tests were conducted in mode I on single edge notched (SEN) specimens. The notches were machined using a high speed steel slit cutter of 0.2 mm thickness. A lathe suitably modified was used for this purpose. The experimental arrangement is shown by a photograph in Fig. 2.1. The fracture toughness for glass fabric reinforced composites was obtained for various test variables as described below:

1. Style of reinforcement

Two different types, A and B, of glass cloth used as described earlier.

2. Ply orientation

0°/90°, plain weave glass cloth
± 45°, plain weave glass cloth

3. Specimen width (w)

w = 15, 25, 35, 40 mm.

4. Initial crack length (a_0)

$\frac{a_0}{w} = 0.1$ to 0.7 in steps of 0.1

5. Specimen length (L)

L = 75, 100 and 150 mm.

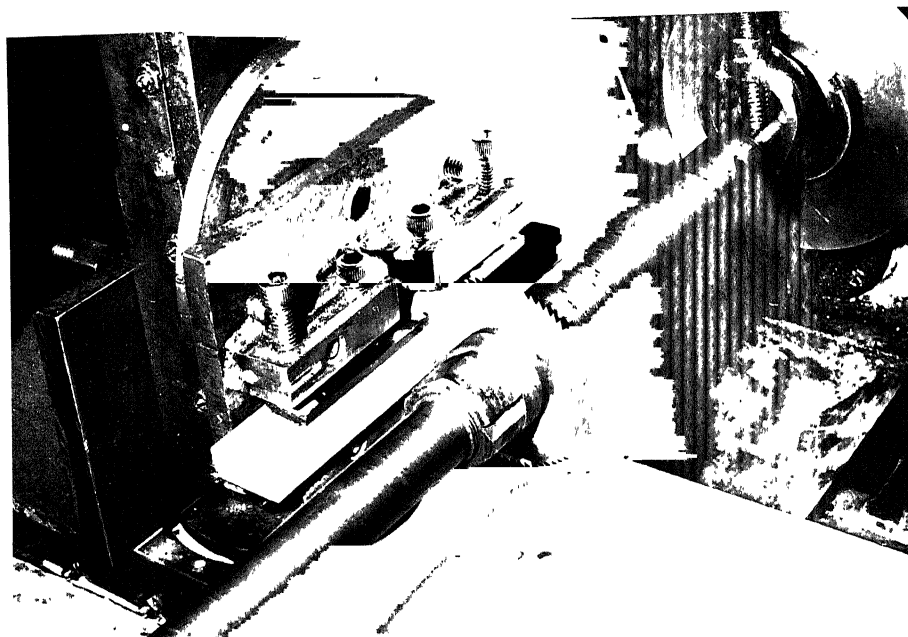


FIG. 2.1 : EXPERIMENTAL ARRANGEMENT
FOR CUTTING NOTCHES

2.2 TESTING SYSTEM:

Fracture toughness tests were conducted on SEN specimens in a 10 Ton MTS (material test system) testing machine. A view of the experimental arrangement is shown in Fig. 2.2. The upper grip is fixed and the lower grip can move in the vertical direction. The tests were conducted in displacement control mode. Instantaneous values of load and displacement of lower grip were recorded on a X-Y recorder. Atleast three specimens were tested for each crack length. A total of over 200 specimens were tested.

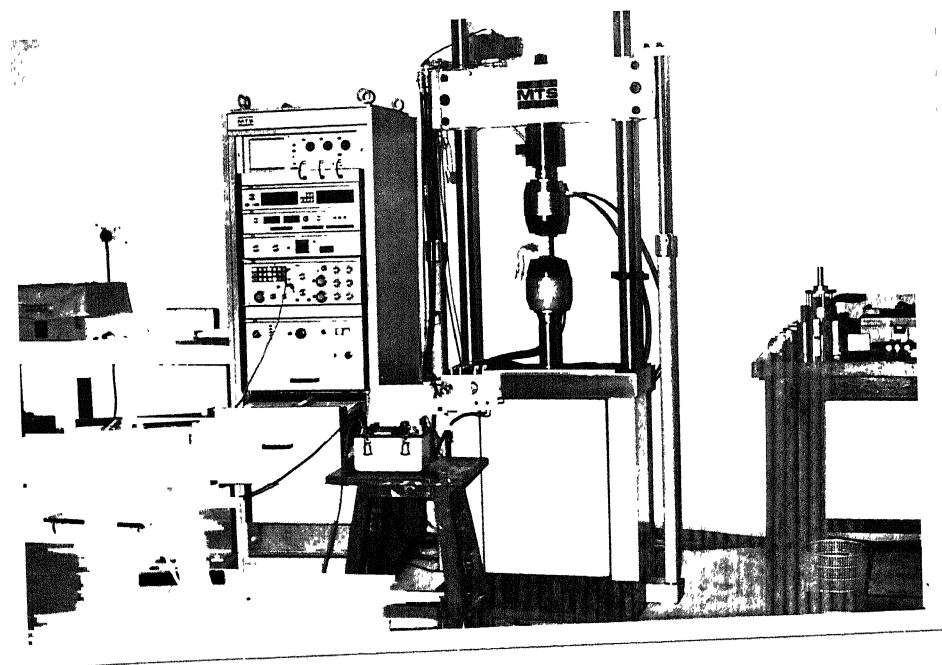


FIG. 2.2 : EXPERIMENTAL ARRANGEMENT
ON MTS MACHINE

CHAPTER-3

EXPERIMENTAL RESULTS AND DISCUSSION

The fracture toughness tests were conducted on (1) $0^\circ/90^\circ$, plain woven cloth laminates and (2) $\pm 45^\circ$, plain woven cloth laminates. The results are discussed individually in this chapter.

3.1 $0^\circ/90^\circ$ PLAIN WOVEN CLOTH LAMINATES:

Laminates with glass cloth reinforcement of two different types as specified in Sec. 2.1 were tested. The stress-strain behaviour of the two types of laminates is shown in Fig. 3.1 and Fig. 3.2 for type A and type B laminates respectively. Their mechanical properties are summarised in Table 3.1.

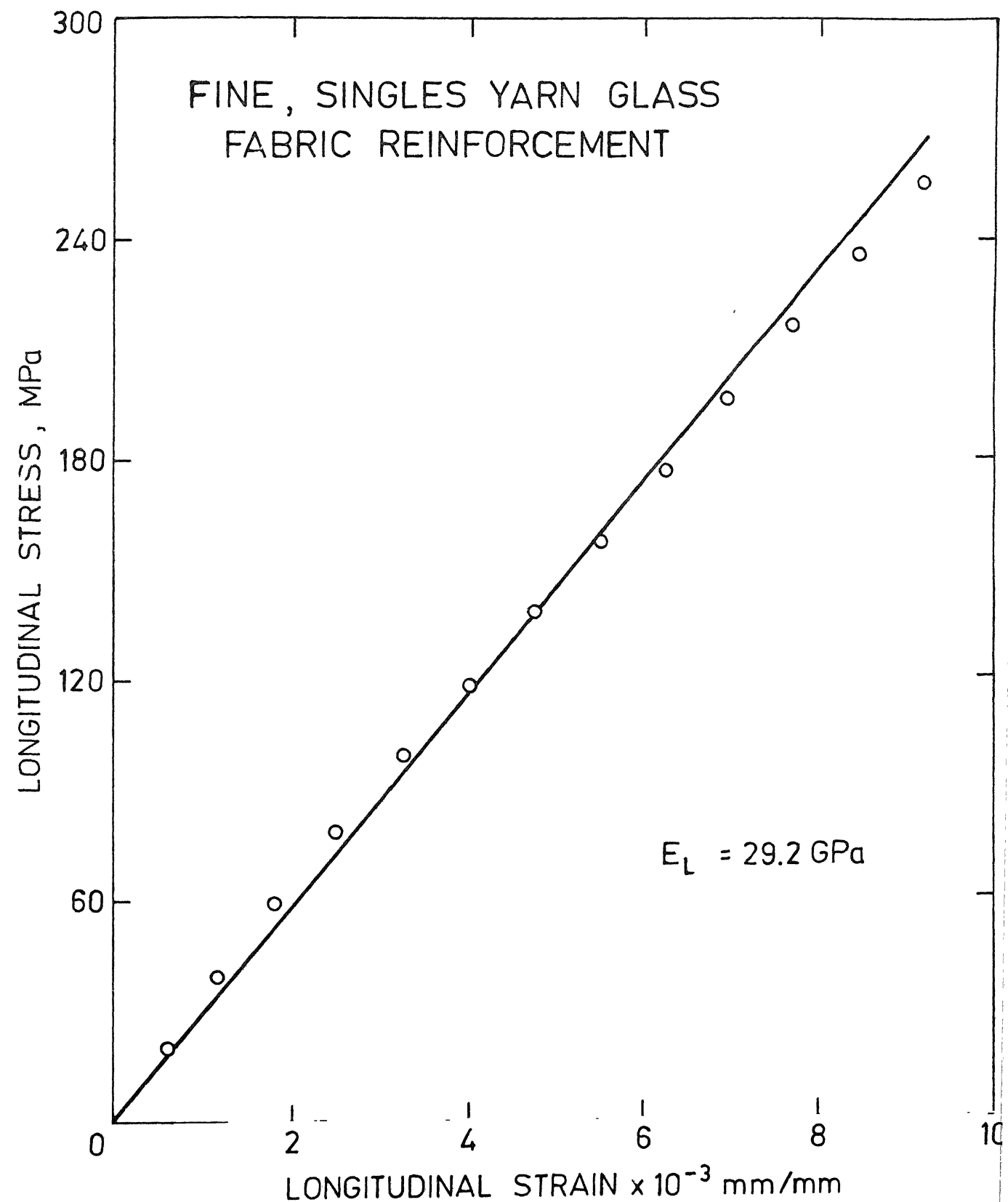


FIG. 3.1 STRESS STRAIN CURVE FOR LAMINATES WITH
TYPE-A REINFORCEMENT.

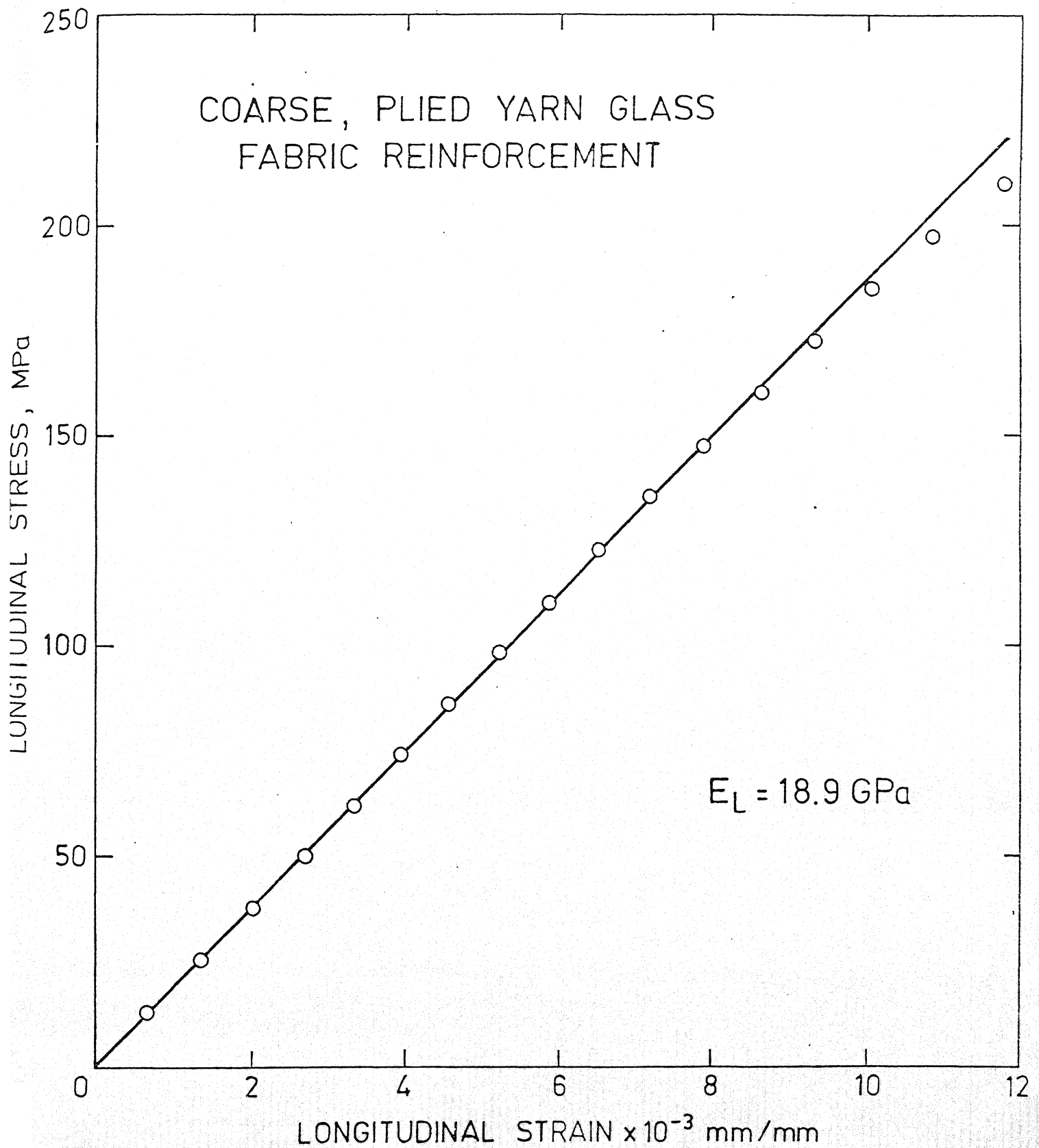


FIG. 3.2 STRESS STRAIN CURVE FOR LAMINATES WITH TYPE-B REINFORCEMENT.

TABLE 3.1

PROPERTY	Laminates with type A reinfor- cement	Laminates with type B reinfor- cement
1. Fiber Volume Fraction, V_f	39.5%	37.5%
2. Modulus of Elasticity		
Longitudinal, E_L	29.2 GPa	18.9 GPa
Transverse, E_T	29.2 GPa	18.9 GPa
3. Ultimate Tensile Strength		
Longitudinal, σ_{LU}	267 MPa	222 MPa
Transverse, σ_{TU}	267 MPa	222 MPa
4. Poisson's Ratio		
ν_{LT}	0.175	0.194
ν_{TL}	0.175	0.194
5. Shear Modulus G_{LT}	4.06 GPa	1.80 GPa

3.1.1 EXPERIMENTAL EVALUATION OF J_{1C} :

Fracture toughness studies have been performed on glass cloth reinforced epoxy resin. From type A and type B laminates specimens 25 mm wide, 100 mm long, 2 mm thick and crack lengths varying between 0.1 and 0.7 of specimen width were tested in displacement control mode. The upper grip is fixed and the lower grip moves with constant rate of displacement (0.33 mm/min.). The MTS grips are inflexible causing uniform displacement along the width of the specimen. A schematic diagram of a SEN specimen showing the imposed displacement boundary conditions and J-integral contour is shown in Fig. 3.3.

Test samples with two different styles of glass fabric reinforcement were studied with an aim to find the more effective reinforcement style, and to find differences in fracture behaviour, if any.

Typical load displacement curves for both types of specimens, with different initial crack lengths are shown in Figs. 3.4 and 3.5. Specimens of both types with small cracks fracture suddenly causing an abrupt drop in load, whereas specimens with larger cracks show a more gradual fracture behaviour. The behaviour is similar to that observed in metals [17] and short fiber composites [18]. This is because the strain

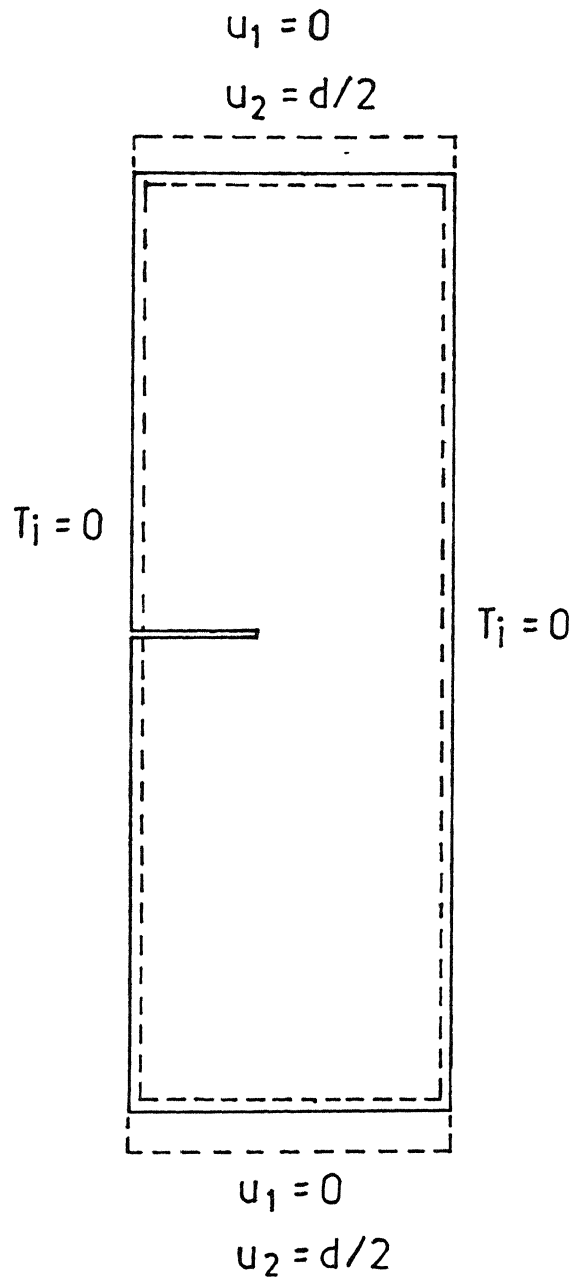


FIG. 3.3 A SEN SPECIMEN SHOWING J-INTEGRAL CONTOUR.

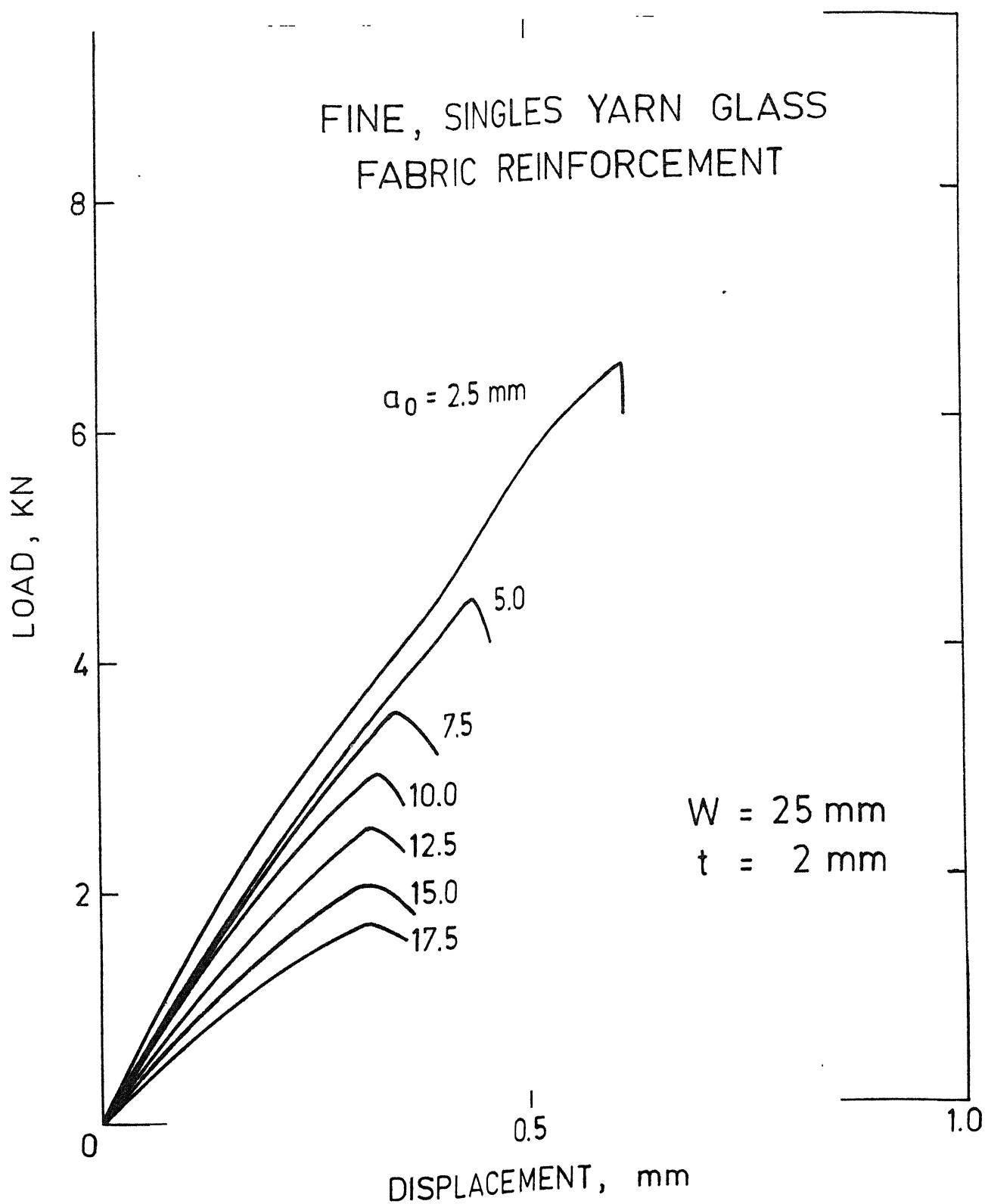


FIG. 3.4 LOAD DISPLACEMENT CURVES FOR 100 mm LONG SPECIMENS WITH TYPE-A REINFORCEMENT.

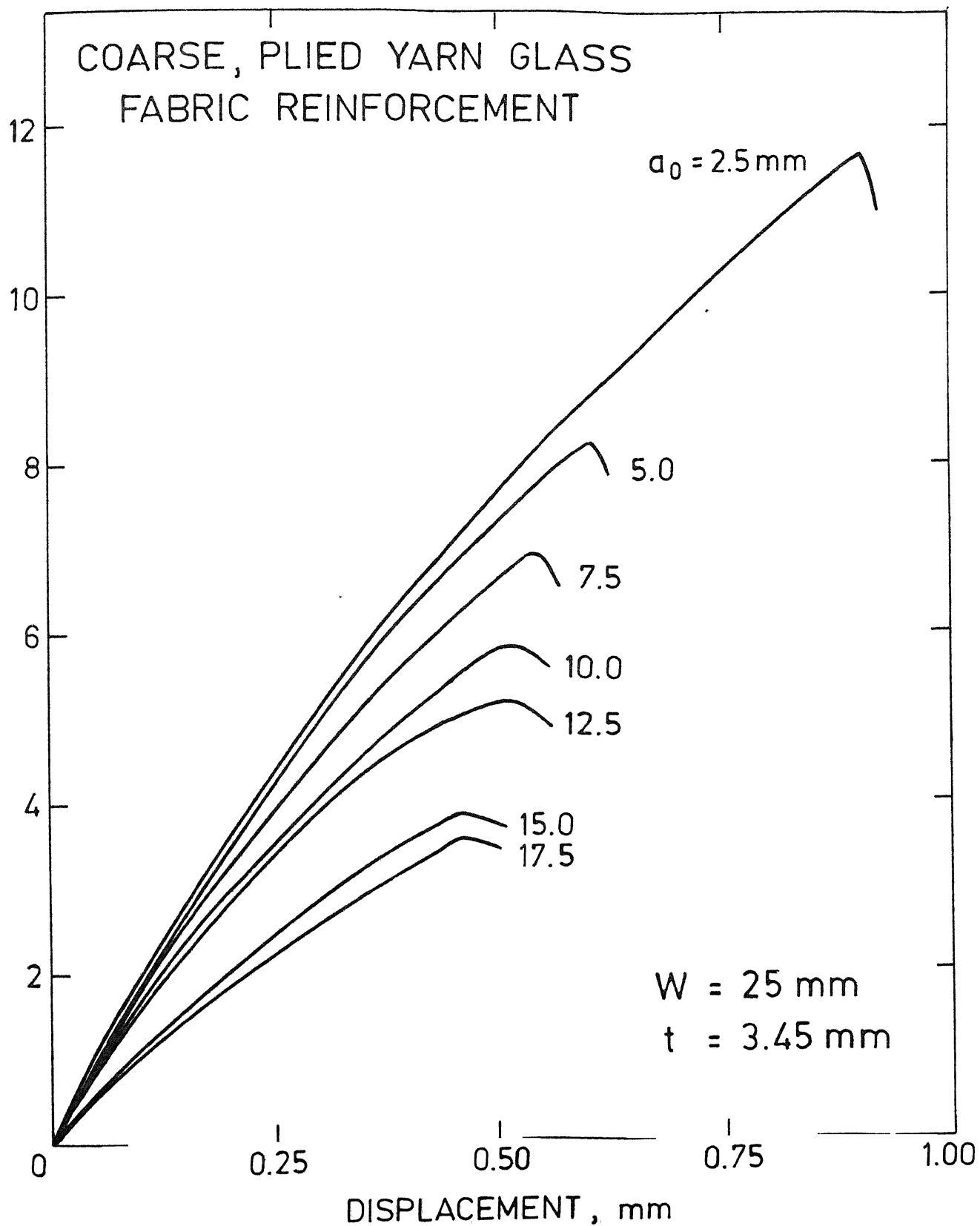


FIG. 3.5 LOAD DISPLACEMENT CURVES FOR 100 mm LONG SPECIMENS WITH TYPE-B REINFORCEMENT.

energy stored during loading in a small crack length specimen is sufficient to cause a catastrophic failure. It is not the case for longer crack length specimens.

The fracture process becomes unstable at a displacement beyond which the load decreases monotonically and the crack grows catastrophically. This displacement is called the critical displacement. It is plotted against crack length in Fig. 3.6 and Fig. 3.7 for both type A and type B specimens. In both cases for small crack lengths the critical displacement decreases with increase in a_0 but remains constant for crack size $a_0/w > 0.5$ or 12.5 mm. The critical value of J-integral is obtained corresponding to the constant critical displacement of 0.29 mm for type A and 0.455 mm for type B as shown in Figs. 3.6 and 3.7. Thus type B laminates deform more before fracture than type A, for the same crack length.

The load displacement curves have been used to obtain the value of J-integral through its energy rate interpretation (Eq. 1.3). To this end, the area under the load displacement curves is obtained graphically to determine the work done in loading the specimen for a given displacement. For each specimen the strain energy per unit thickness is obtained for displacements at

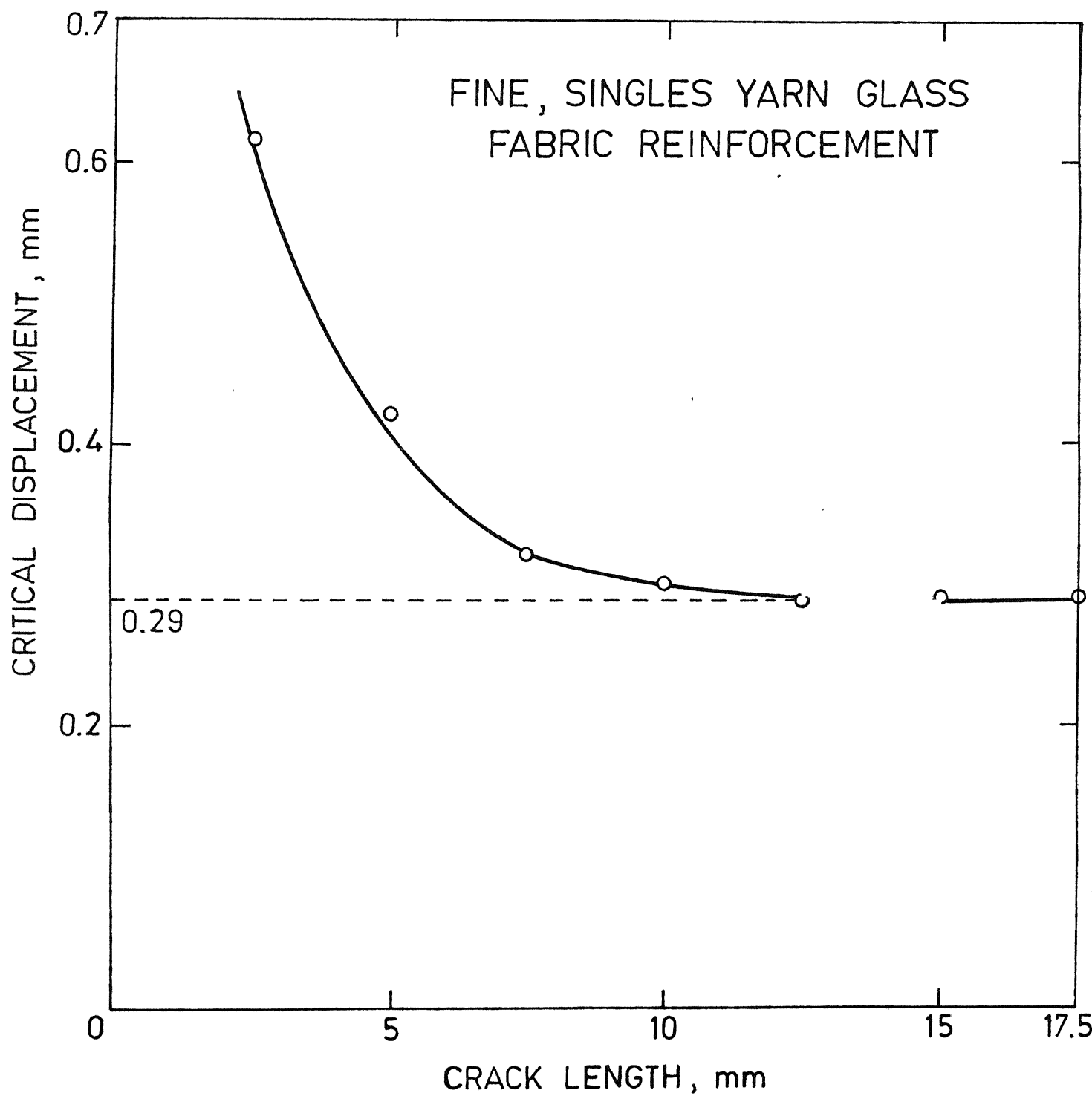


FIG. 3.6 VARIATION OF CRITICAL DISPLACEMENT WITH CRACK LENGTH FOR TYPE-A REINFORCEMENT.

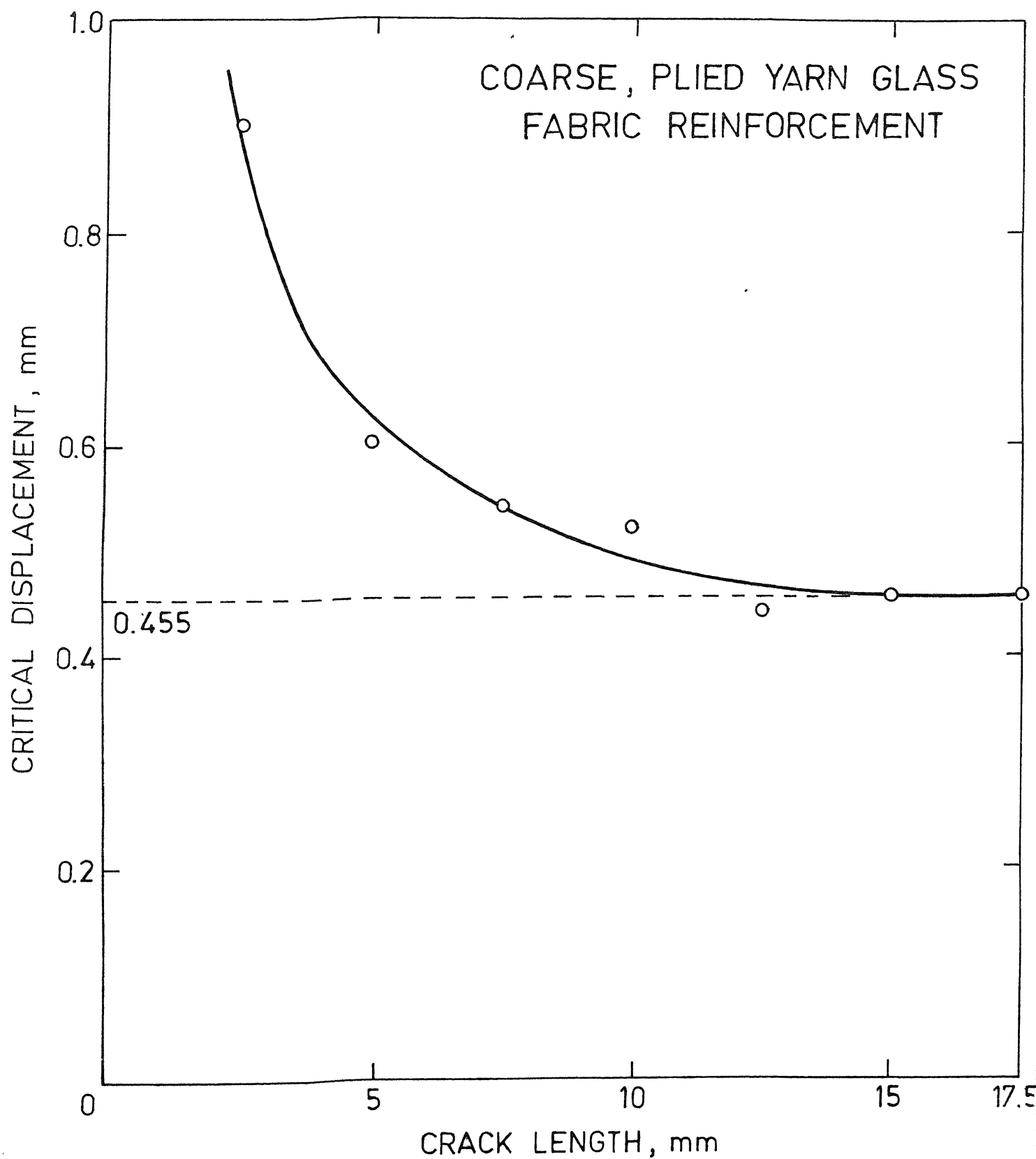


FIG. 3.7 VARIATION OF CRITICAL DISPLACEMENT WITH CRACK LENGTH FOR TYPE-B REINFORCEMENT.

intervals of 0.05 mm. It is plotted in Fig. 3.8 and Fig. 3.9 for both type A and type B specimens respectively, as a function of crack length for different displacements. For a given displacement, the energy absorbed by a specimen decreases as the crack length increases because smaller loads are required. The variation in energy absorbed is less for cracks shorter than 12.5 mm compared to that for longer cracks. This is because in specimens with longer cracks the energy absorbed is essentially in the vicinity of the crack tip and is thus, strongly influenced by crack length.

The J-integral is obtained through slopes of the energy curves in Figs. 3.8 and 3.9. The energy curves in both these figures are approximated by two straight lines. We can thus obtain two J-integral versus displacement plots; one for lower range of crack lengths and another for higher range of crack lengths. The critical displacement for cracks longer than 12.5 mm or $a_0/w > 0.5$ is constant. The variation of J with displacement for cracks longer than 12.5 mm is shown in Fig. 3.10 and Fig. 3.11 for type A and type B specimens respectively. The critical value of J, J_{1C} , corresponds to the constant value of critical displacement. For type A specimens J_{1C} is 12.8 KJ/m^2 corresponding to a critical displacement of 0.29 mm. For type B

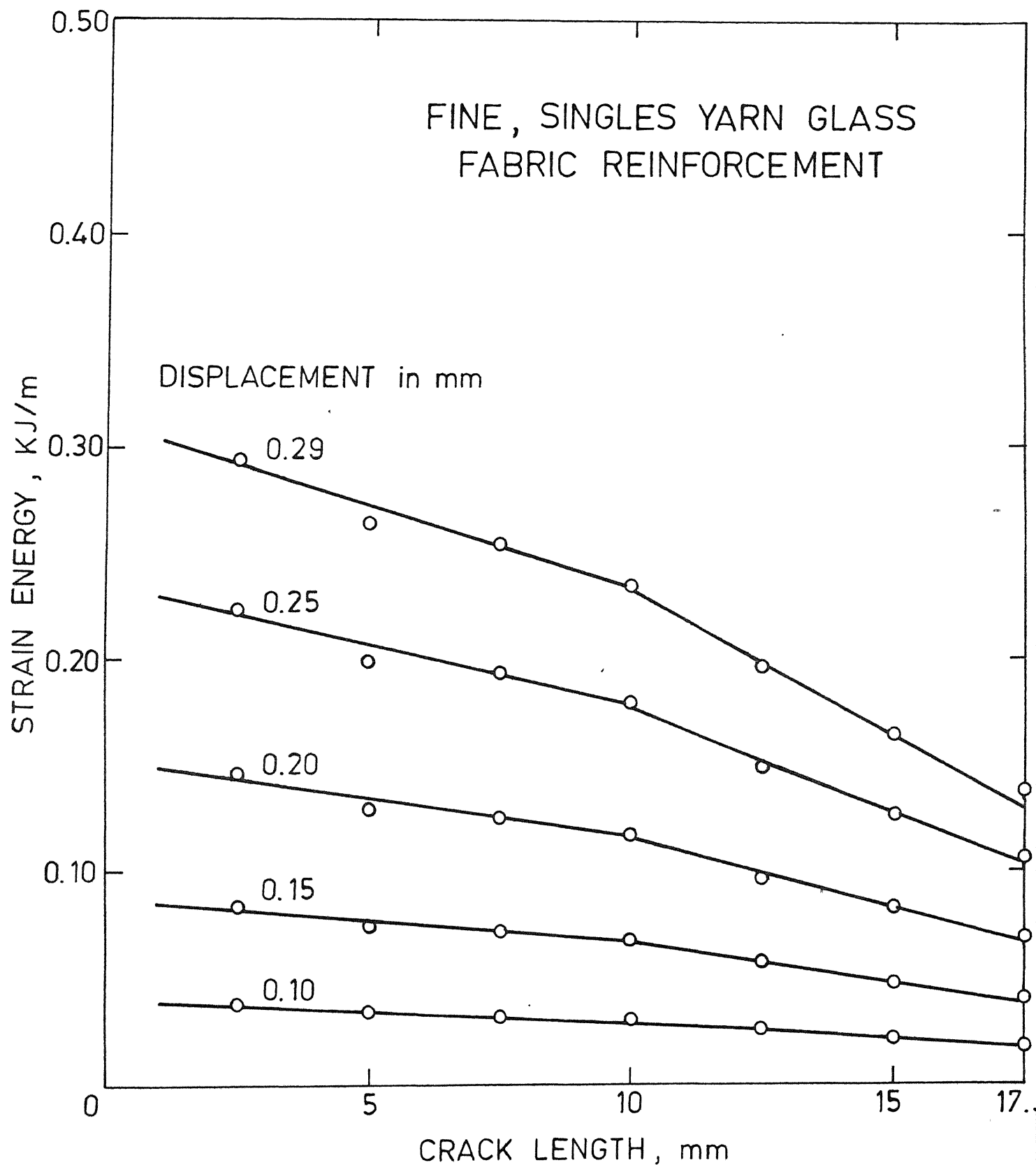


FIG. 3.8 STRAIN ENERGY PER UNIT THICKNESS FOR DIFFERENT DISPLACEMENTS FOR 100 mm LONG SPECIMENS WITH TYPE-A REINFORCEMENT.

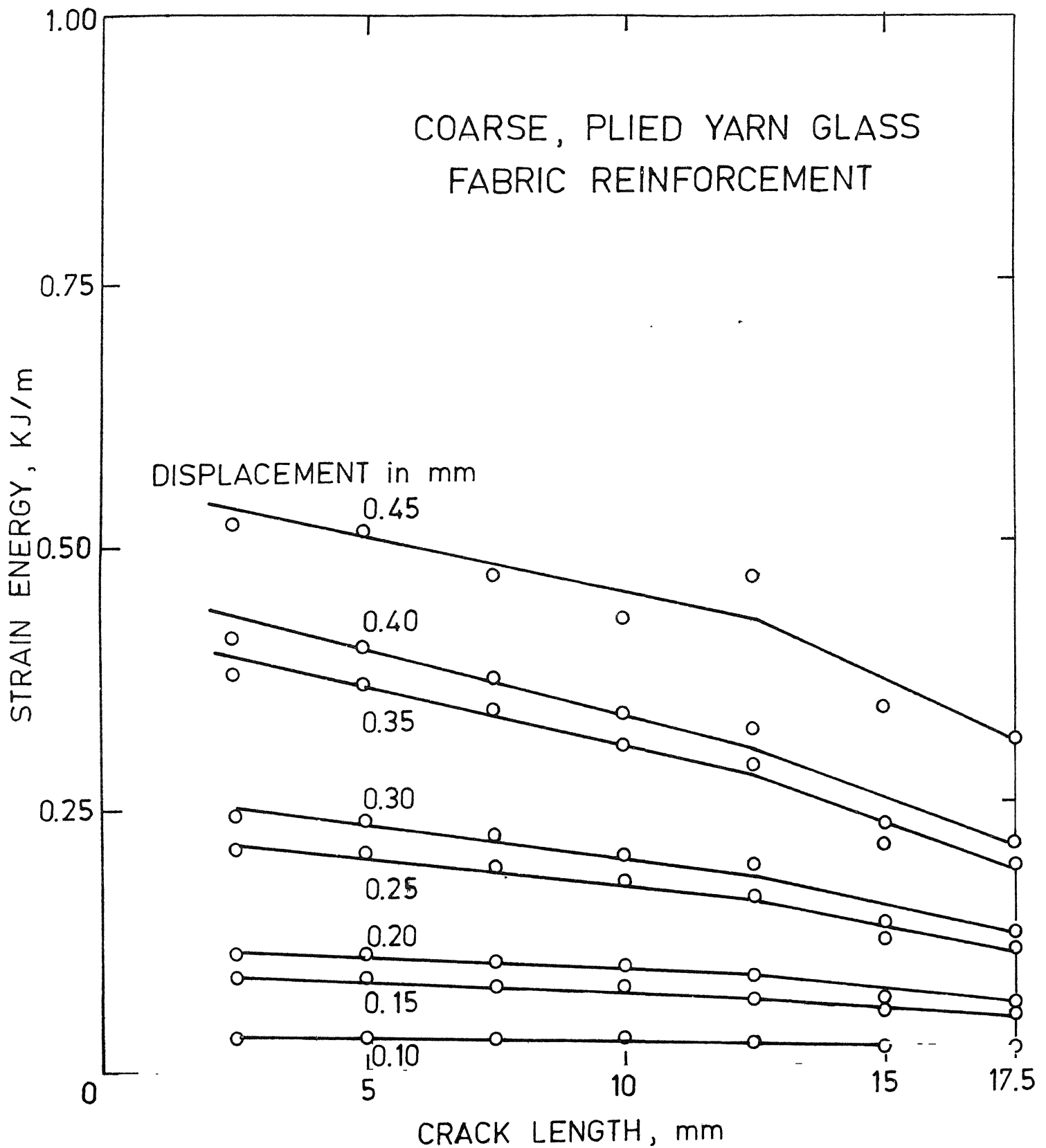


FIG. 3.9 STRAIN ENERGY PER UNIT THICKNESS FOR DIFFERENT DISPLACEMENT FOR 100 mm LONG SPECIMENS WITH TYPE-B REINFORCEMENT.

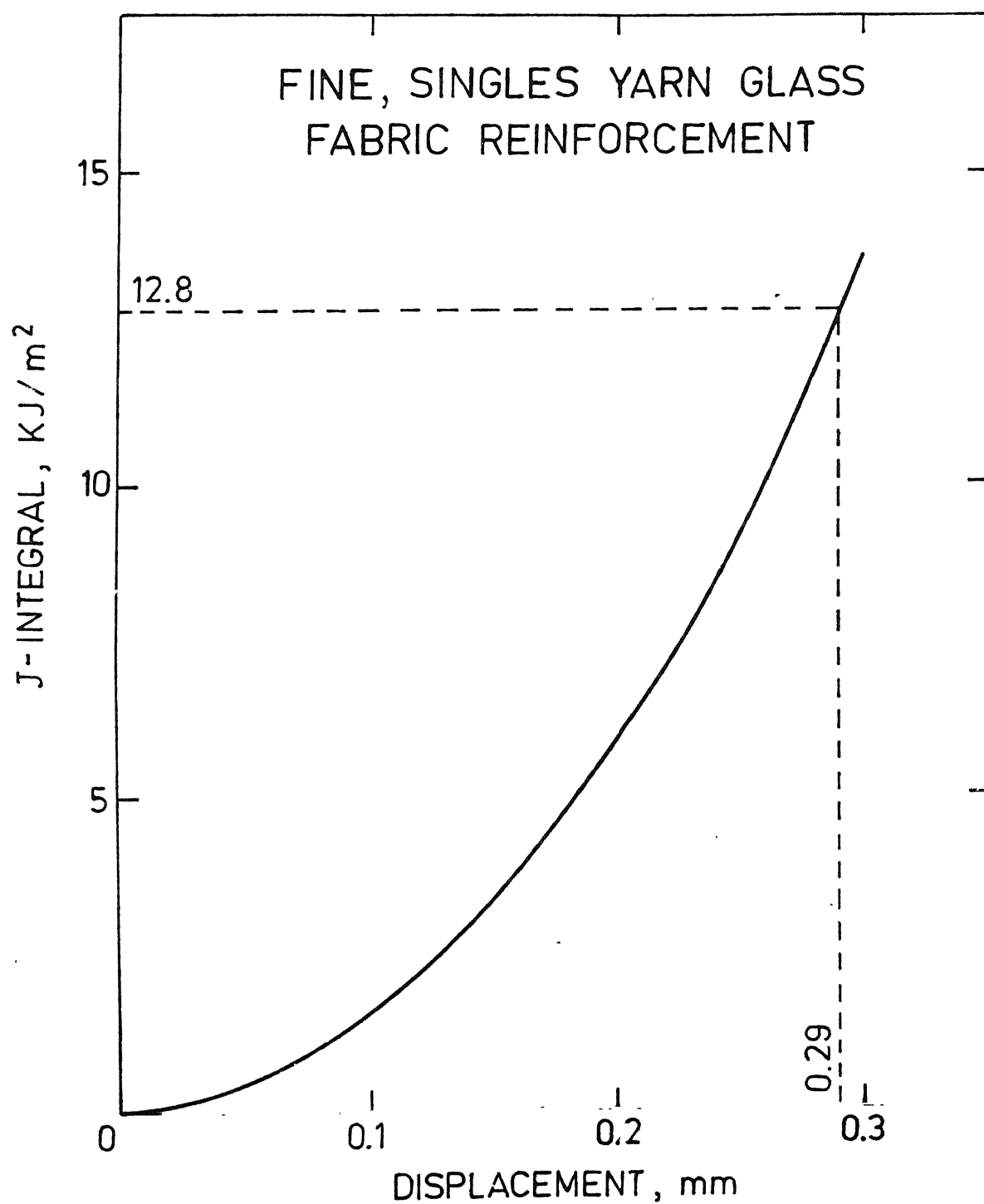


FIG. 3.10a J-INTEGRAL CURVE FOR 100 mm LONG SPECIMENS WITH TYPE-A REINFORCEMENT FOR $a_0/W > 0.5$.

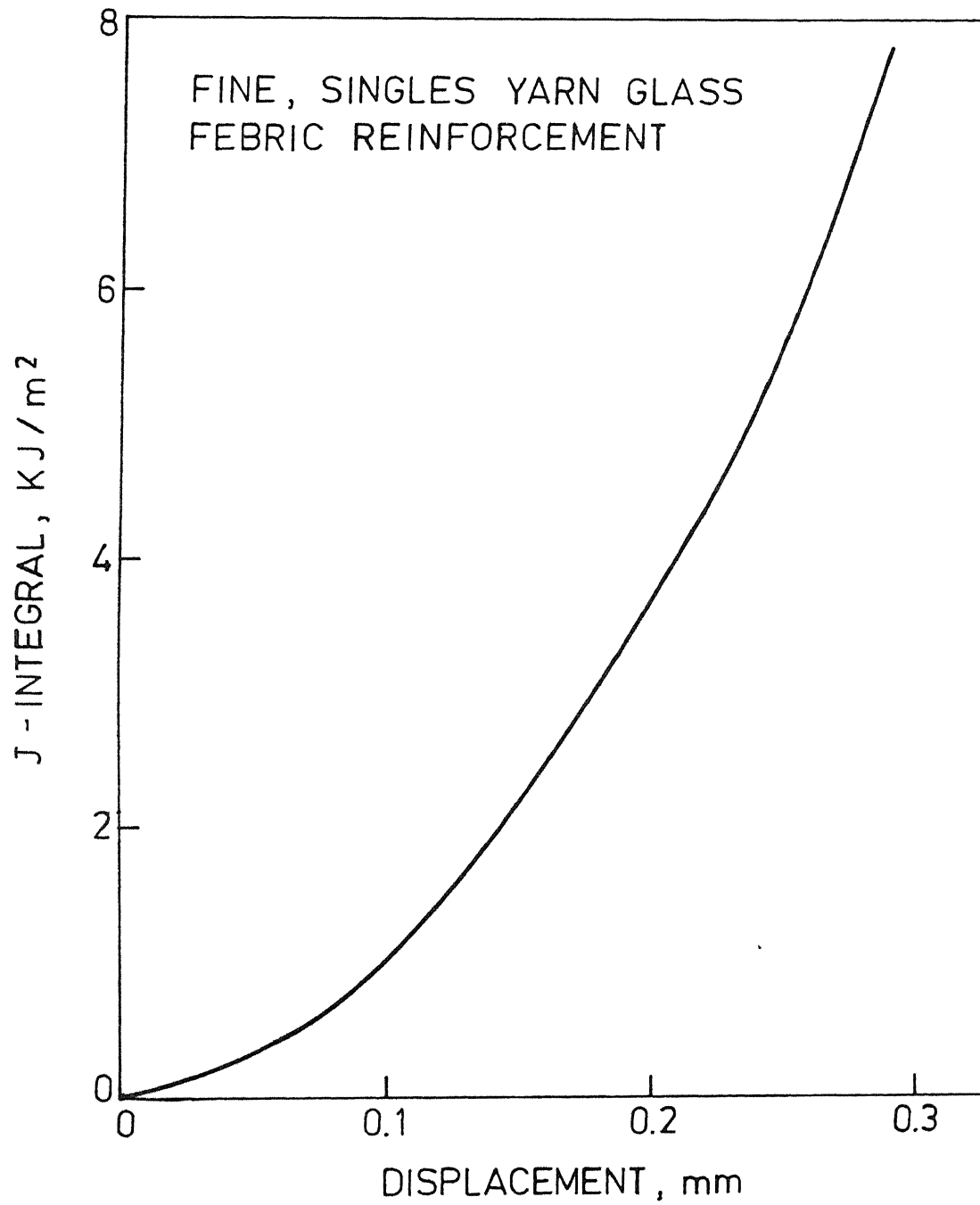


FIG. 3.10 b J - INTEGRAL CURVE FOR 100 mm LONG SPECIMENS TYPE - A REINFORCEMENT FOR $a_0/w < 0.4$.

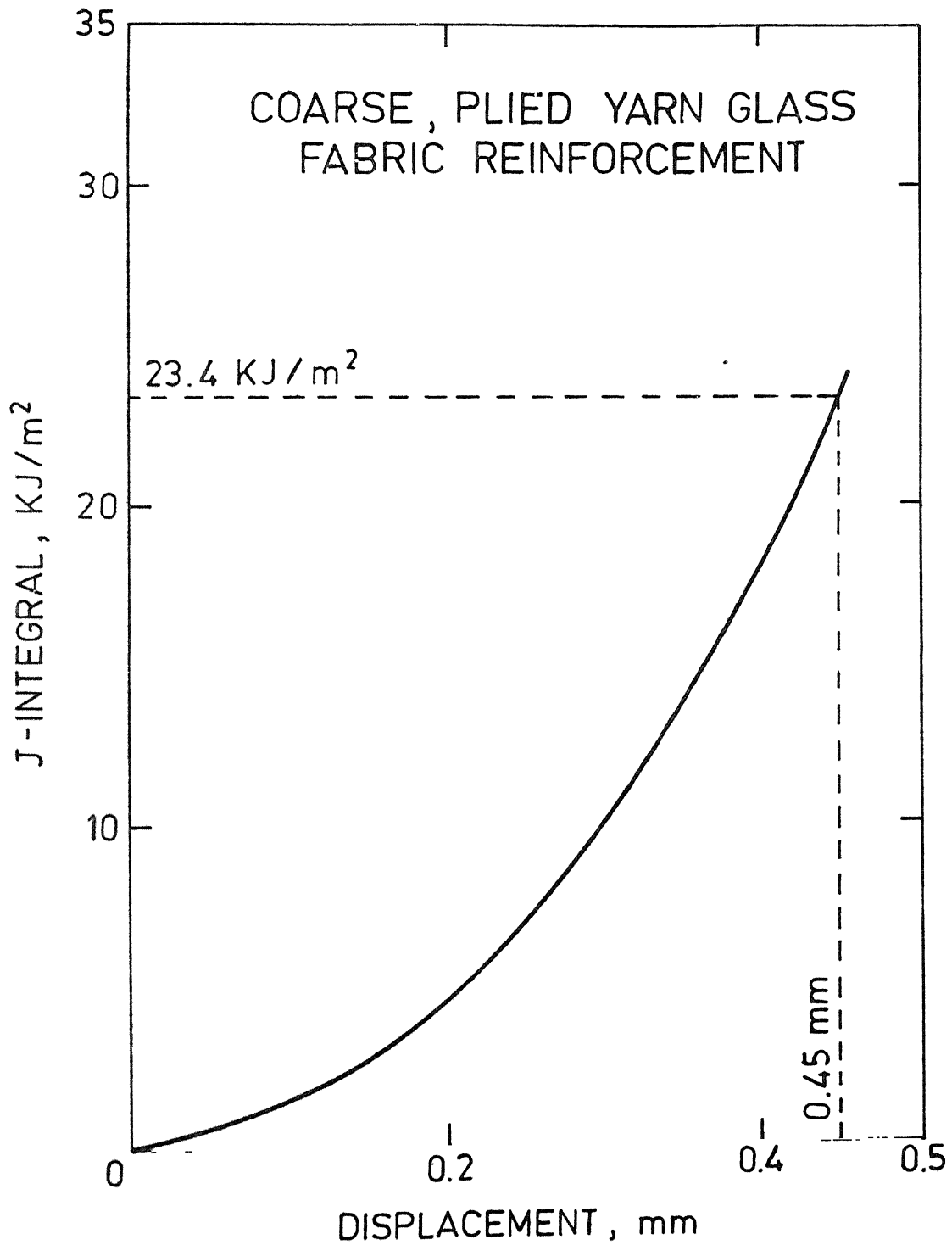


FIG. 3.11a J-INTEGRAL CURVE FOR 100 mm LONG SPECIMENS WITH TYPE-B REINFORCEMENT FOR $a_0/W > 0.5$

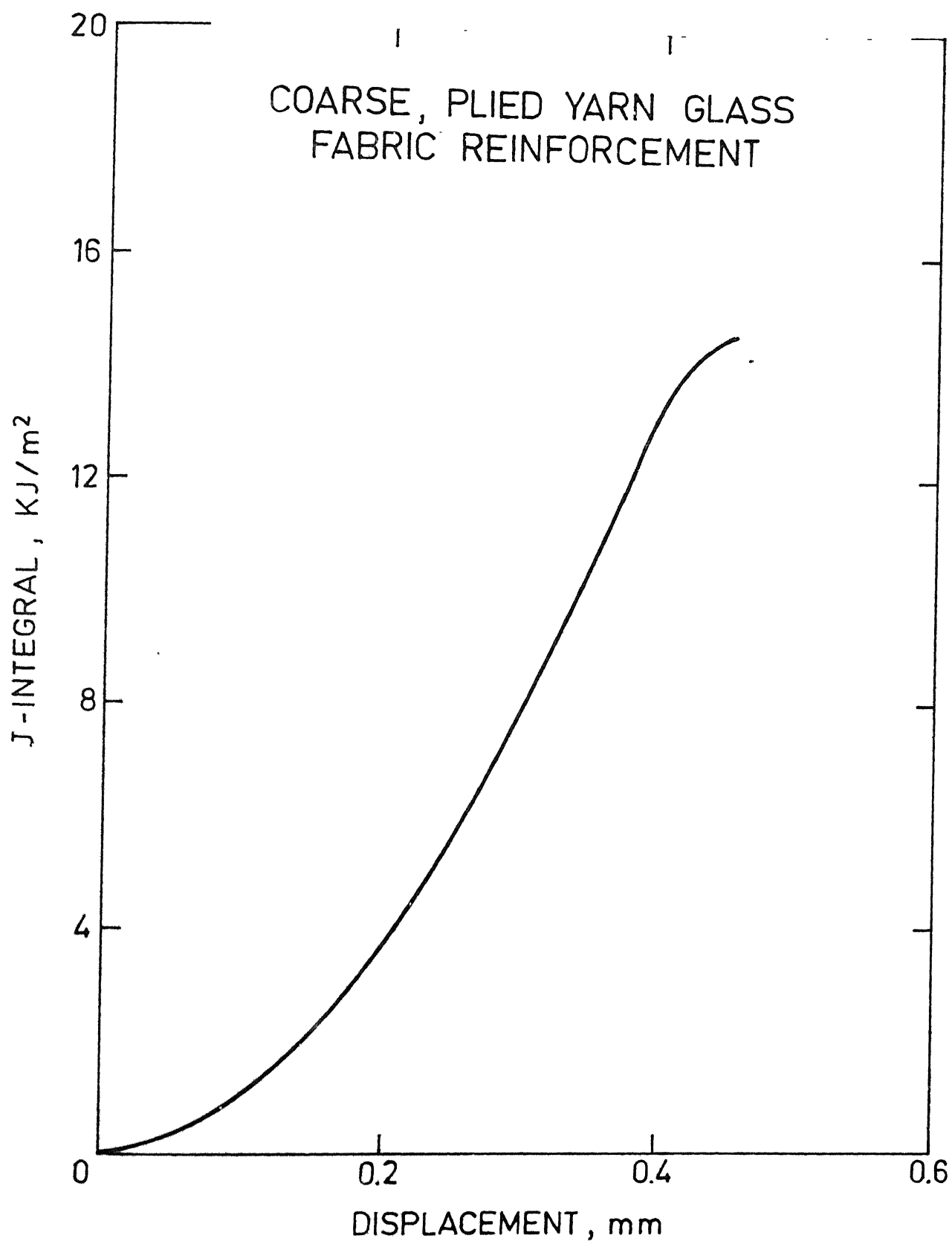


FIG. 3.11b J-INTEGRAL CURVE FOR 100 mm LONG SPECIMENS WITH TYPE-B REINFORCEMENT FOR $a_0/W < 0.5$

specimens J_{1C} is 23.4 KJ/m^2 corresponding to a critical displacement of 0.455 mm . Thus for nearly equal volume fractions a substantially larger value of J_{1C} is obtained for specimens with type-B glass fabric reinforcement. The possible reasons for a higher value of J critical in type B specimens are discussed in Sec. 3.1.4.

For cracks less than 12.5 mm or $a_0/w < 0.5$ the critical displacement is more than the constant value of critical displacement obtained for $a_0/w > 0.5$, and increases with crack length. Hence a critical value of J cannot be determined uniquely for lower ranges of crack length. The applicability of J -integral in this range is discussed in the next section.

From the previous discussion it is seen that when the crack size is equal to or longer than 12.5 mm or $a_0/w \geq 0.5$ the fracture behaviour is governed essentially by the crack tip environment. This results in a constant critical displacement and a unique value of J -integral. For these crack lengths the fracture load is small, which does not result in any material damage away from the crack tip region. On the other hand when cracks are small ($a_0 < 12.5 \text{ mm}$ or $a_0/w < 0.5$), the J -integral and critical displacement depends on the crack length. This indicates that in addition to the

crack tip environment, the region away from it also influences such quantities as energy absorbed and displacement at fracture. This may be attributed to the fracture load being high enough to cause general material damage.

3.1.2 EFFECT OF SPECIMEN LENGTH:

In order to study the influence of general material damage away from the crack tip in specimens with smaller cracks, additional specimens with varying lengths were tested. The load displacement records for specimens with type A and type B reinforcement are shown in Fig. 3.12-3.13 and Fig. 3.14-3.15 for $L = 75$ mm and $L = 150$ mm, respectively. The critical displacements for specimens with different initial crack lengths are plotted against specimen length in Fig. 3.16 and Fig. 3.17 for type A and type B laminates respectively. As expected, the critical displacement increases with specimen length for all crack lengths. And the rate of increase of critical displacement is higher for specimens with smaller crack lengths. For longer cracks the straight lines overlap. This is consistent with figs. 3.15 and 3.17.

For smaller crack lengths, the total displacement of the specimen is the sum of the displacement in

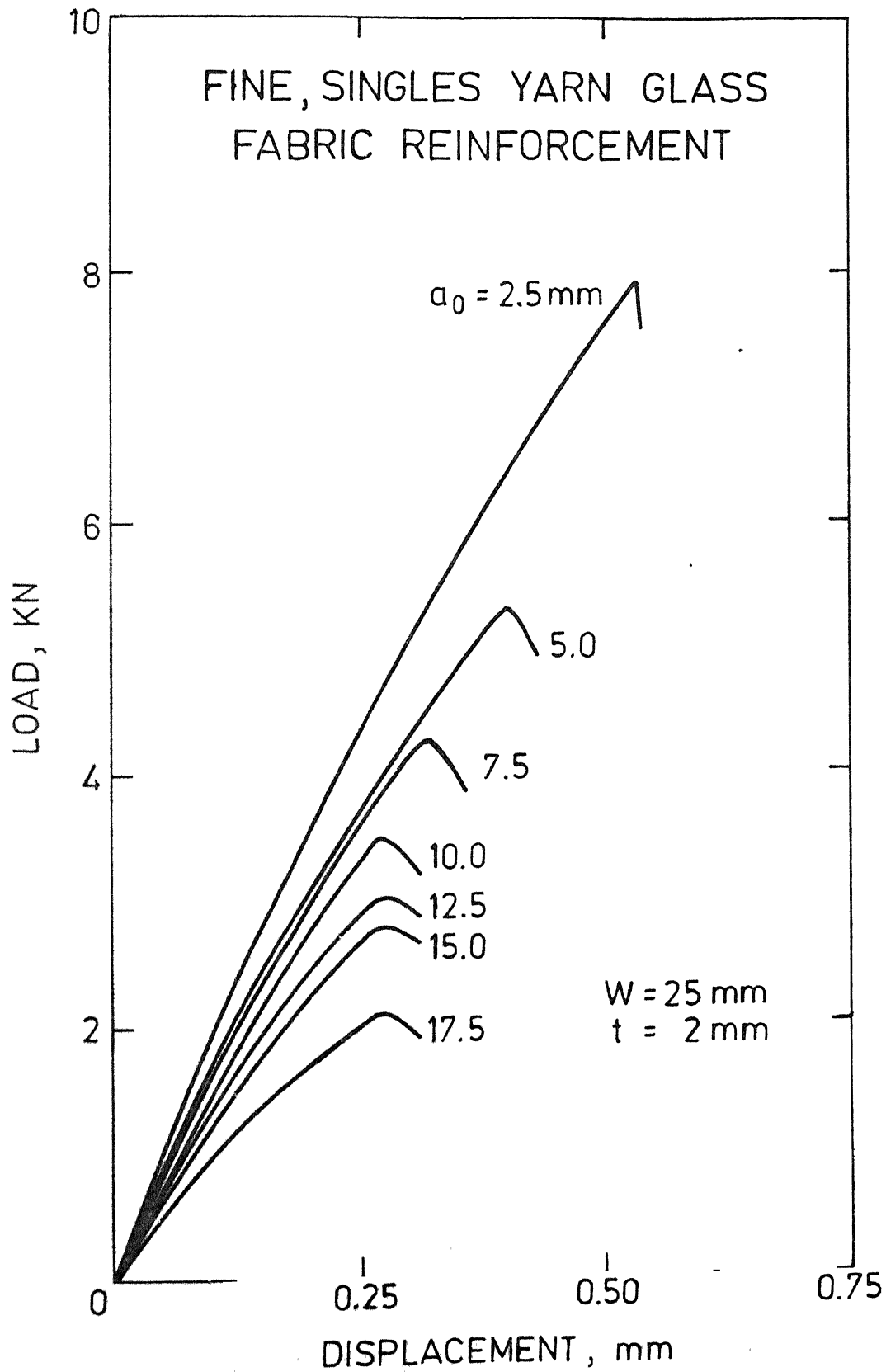


FIG. 3.12 LOAD DISPLACEMENT CURVES FOR 75 mm
LONG SPECIMENS FOR TYPE-A REINFORCEMENT.

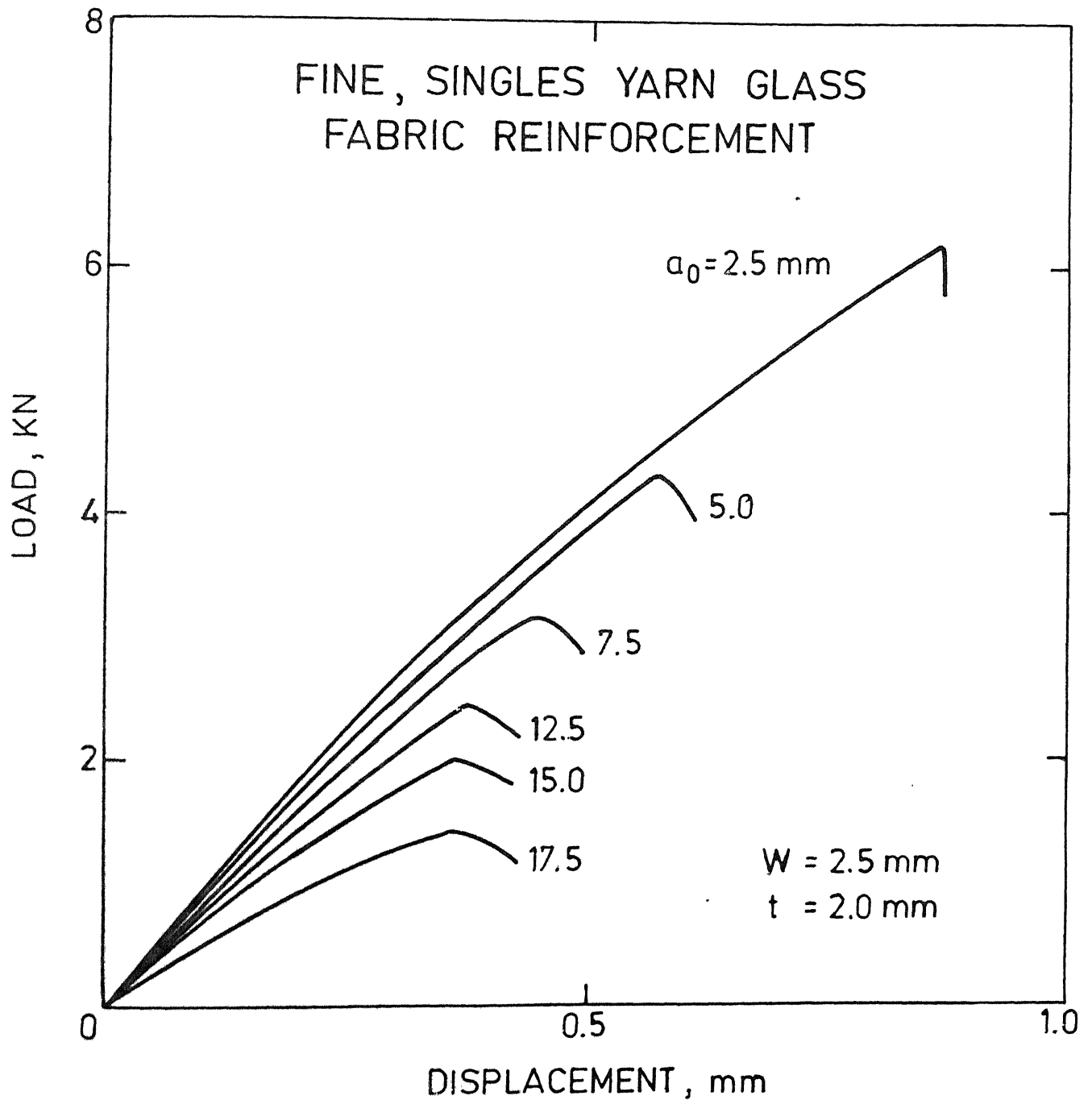


FIG. 3.13 LOAD DISPLACEMENT CURVES FOR 150 mm LONG SPECIMENS FOR TYPE-A REINFORCEMENT.

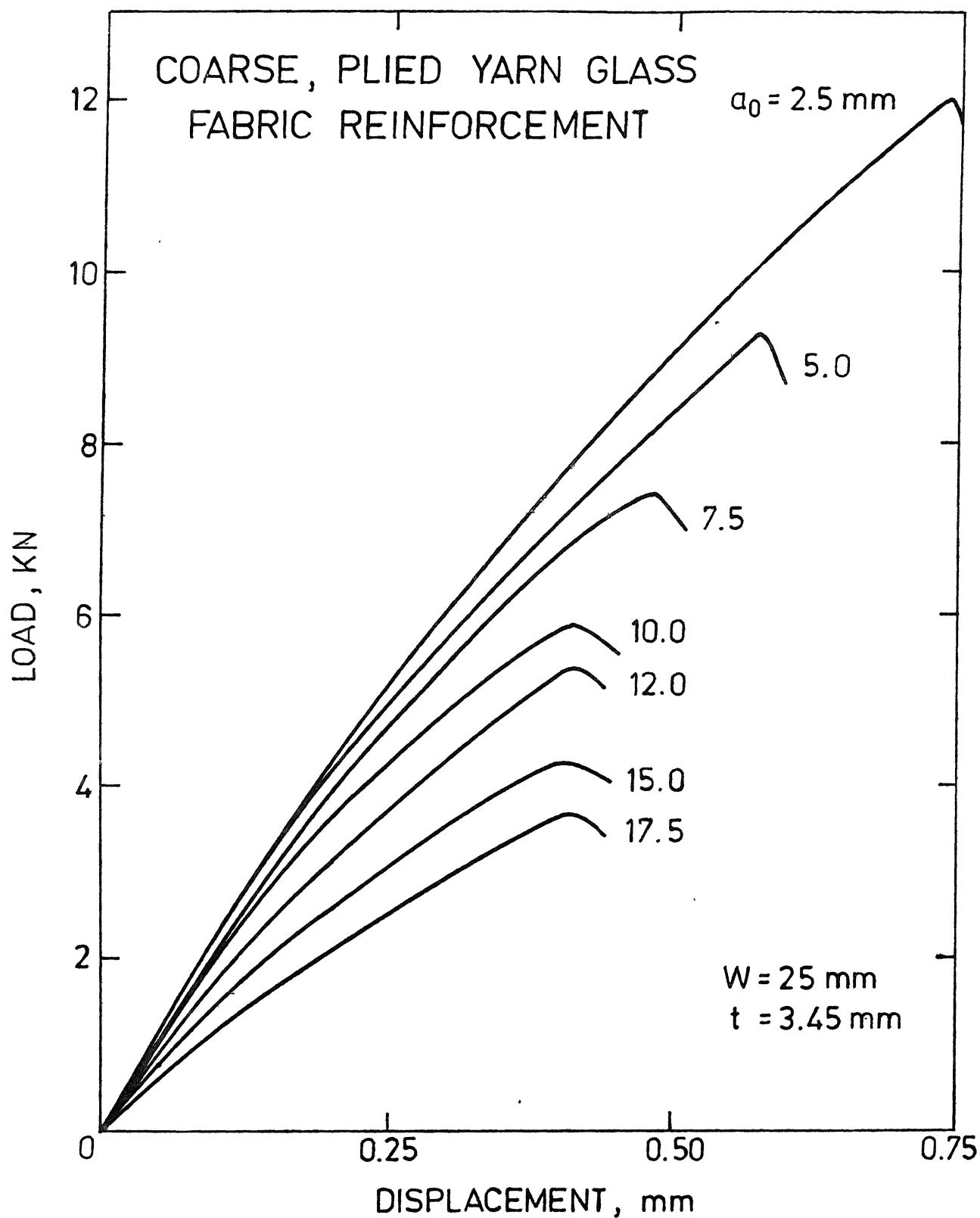


FIG. 3.14 LOAD DISPLACEMENT CURVES FOR 75 mm LONG SPECIMENS WITH TYPE-B REINFORCEMENT.

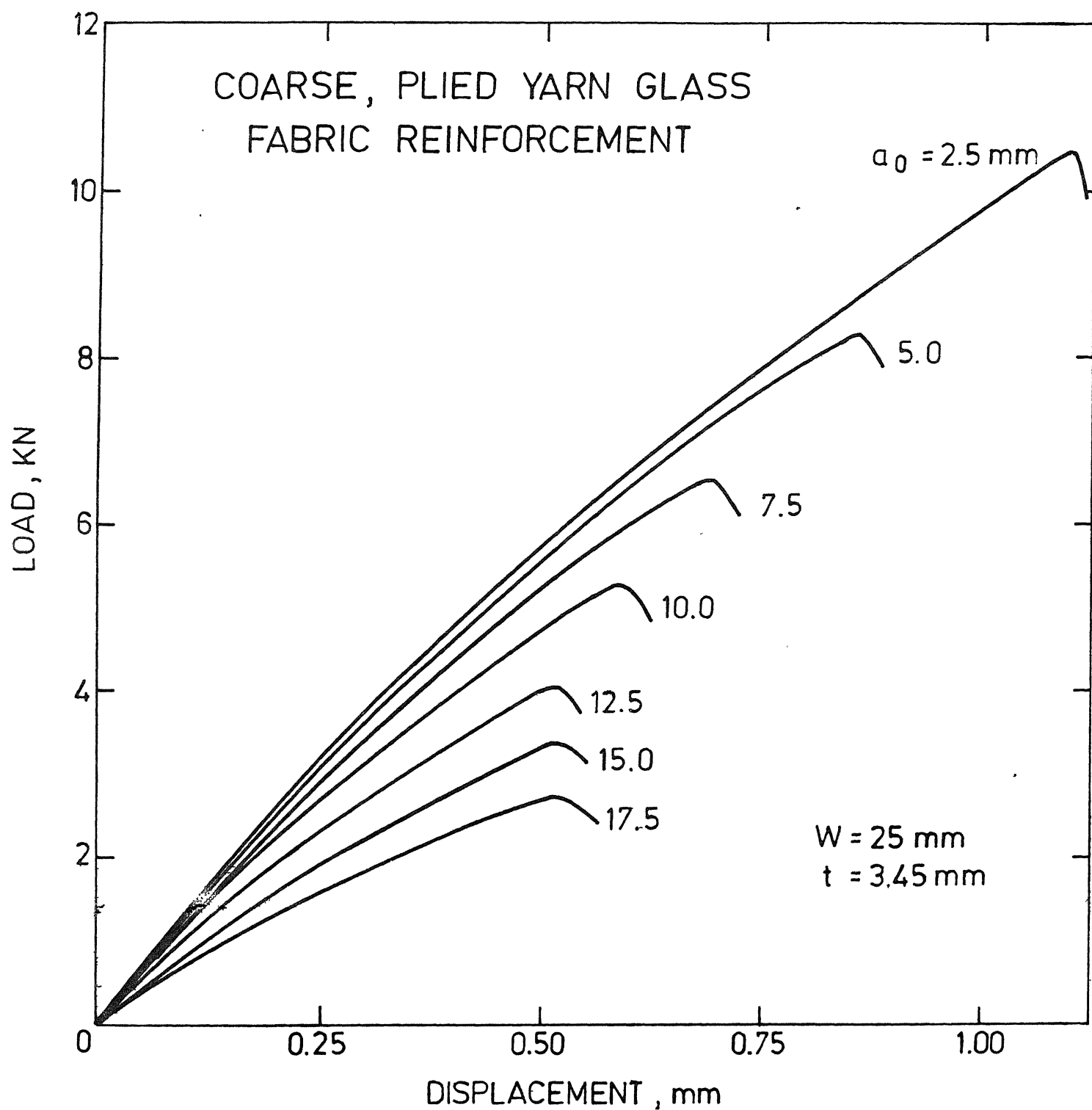


FIG. 3.15 LOAD DISPLACEMENT CURVES FOR 150 mm LONG SPECIMENS WITH TYPE-B REINFORCEMENT.

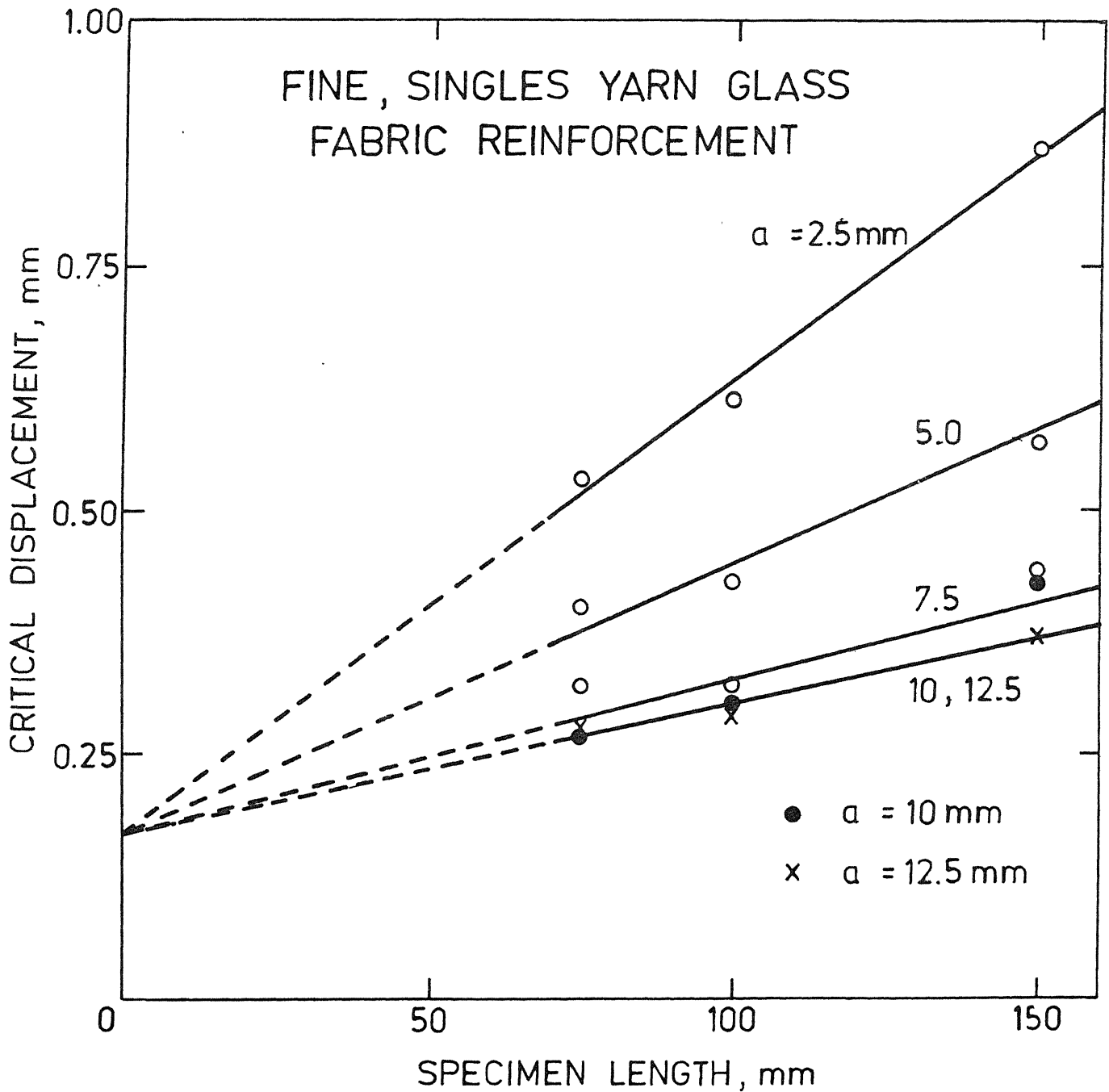


FIG. 3.16 VARIATION OF CRITICAL DISPLACEMENT WITH SPECIMEN LENGTH FOR DIFFERENT INITIAL CRACK LENGTH FOR TYPE-A REINFORCEMENT.

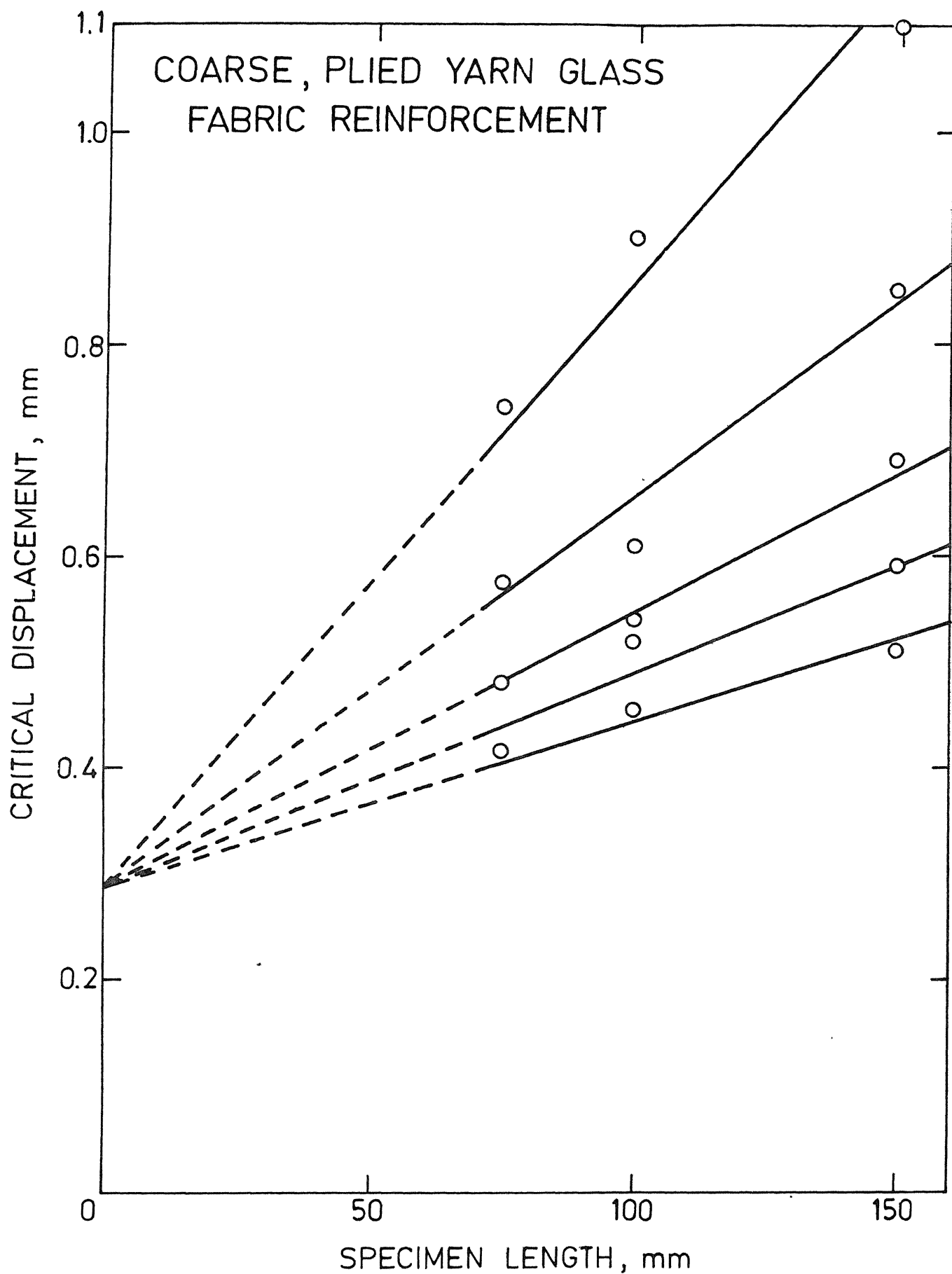


FIG. 3.17 SPECIMEN LENGTH VS CRITICAL DISPLACEMENT
FOR DIFFERENT INITIAL CRACK LENGTH FOR
TYPE-B REINFORCEMENT.

the crack tip region, and displacement in the region away from it, which should be a function of specimen length. The intercept on the ordinate obtained through extrapolation of a straight line in Fig. 3.16 may be regarded as the displacement in the crack tip region alone. Interestingly all the straight lines in fig.3.16 and fig. 3.17 intercept the ordinate at the same point. This common intercept may be regarded as a critical displacement due to the presence of the crack and whose value is independent of crack length and specimen length.

Variations of energy absorbed upto fracture are shown in Fig. 3.18 and Fig. 3.19 for type-A and type-B reinforcements respectively, for different crack lengths. The total energy absorbed may be thought of as the sum of the energies absorbed in the crack tip region and away from it. The energy absorbed in the crack tip region depends on the crack length whereas the energy absorbed in the region away from it depends on the specimen length. It is observed that for cracks larger than $a_0/w \geq 0.5$, the energy absorbed is independent of the specimen length, signifying negligible energy absorption in the region away from the crack tip. The variation of J with displacement for cracks larger than 12.5 mm for different specimen lengths is

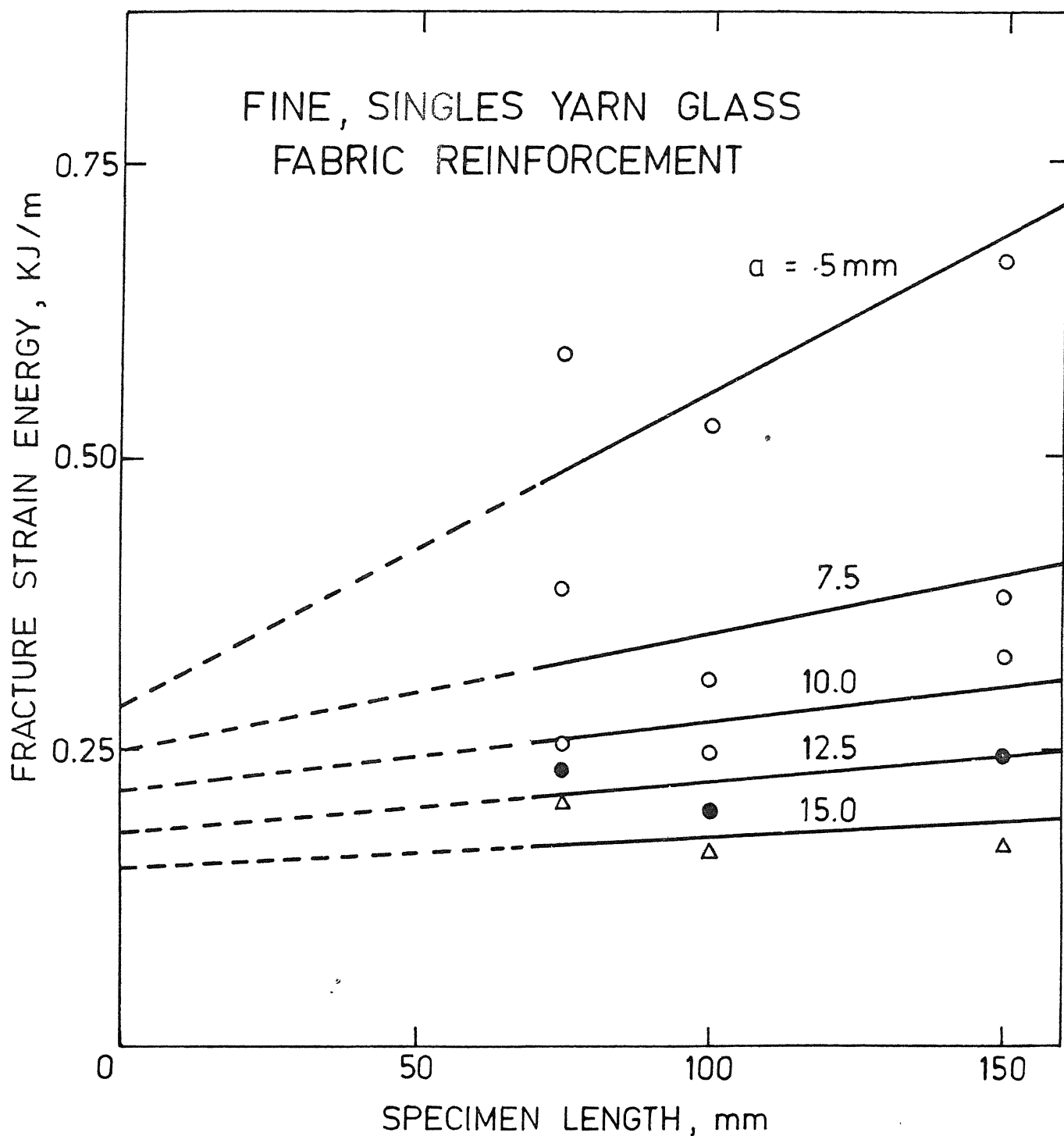


FIG. 3.18 VARIATION OF FRACTURE STRAIN ENERGY WITH SPECIMEN LENGTH FOR DIFFERENT INITIAL CRACK LENGTHS FOR SPECIMENS WITH TYPE-A REINFORCEMENT.

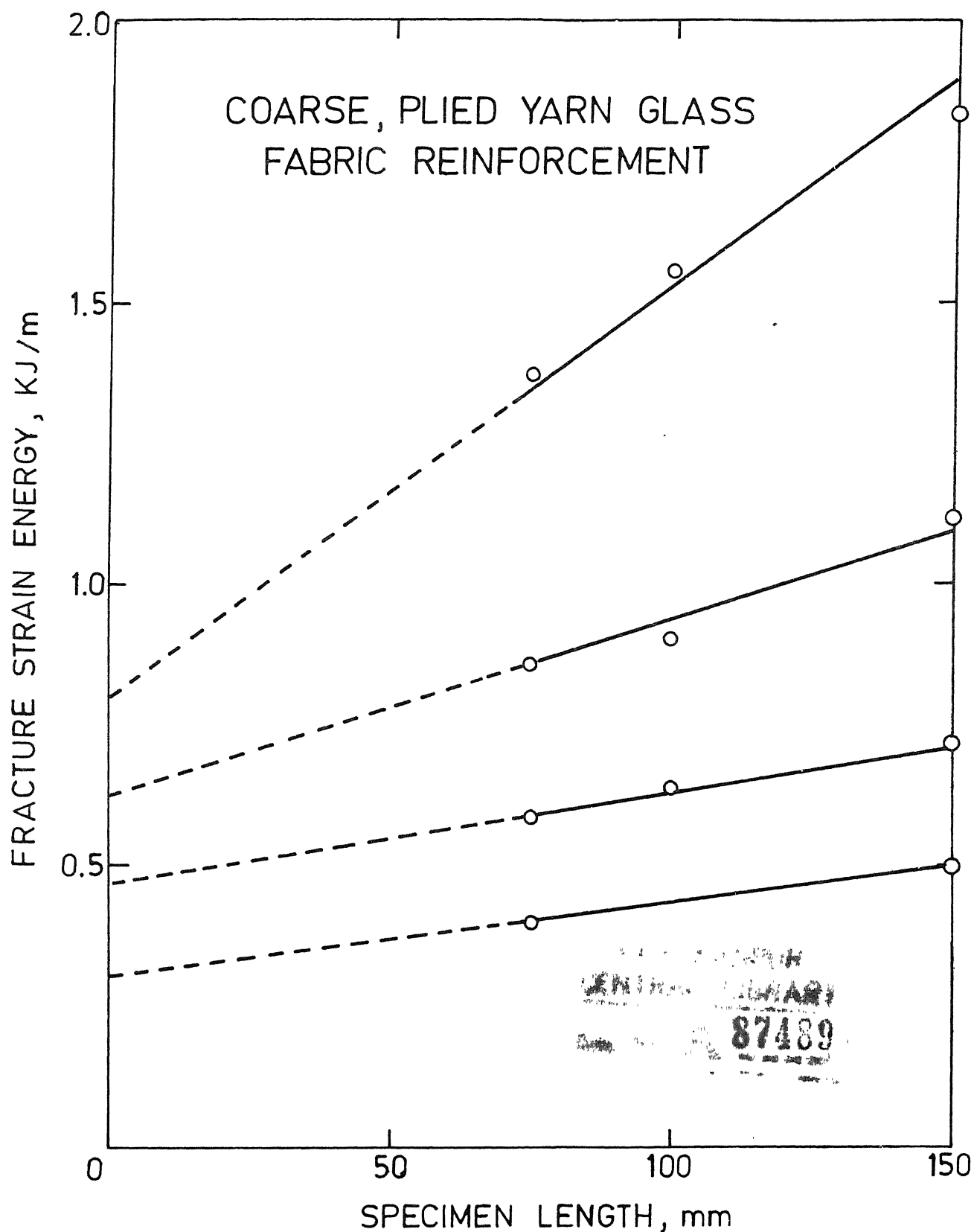


FIG. 3.19 VARIATION OF FRACTURE STRAIN ENERGY WITH SPECIMEN LENGTH FOR DIFFERENT INITIAL CRACK LENGTHS FOR SPECIMENS WITH TYPE-B REINFORCEMENT.

shown in Fig. 3.20 and Fig. 3.21 for type A and type B specimens respectively. The critical value of J corresponds to the critical displacement for a particular specimen length. The J_{1C} values thus obtained are plotted against specimen length in Fig. 3.22 and Fig. 3.23 for type A and type B reinforcement respectively. It is observed that J_{1C} is independent of specimen length, for cracks larger than $a_0/w \geq 0.5$ for both types of specimens. The values of J_{1C} are 12.7 KJ/m^2 for type A laminates and 22.6 KJ/m^2 for type B laminates.

Thus it is seen that the fracture behaviour exhibited by laminates with type-A or type-B reinforcement is similar. The difference however, occurs in the values of fracture toughness; laminates with type-B reinforcement exhibiting substantially higher values of J_{1C} , compared to laminates with type A reinforcement, for nearly same volume fraction. The possible reasons for this are given in a different section. From now onwards we will focus our attention on laminates with type A reinforcement. The fracture behaviour of type A laminates will also hold for other types of glass fabric reinforcements, for different testing variables like length, width and ply orientation.

For cracks less than 12.5 mm or $a_0/w < 0.5$ the total energy absorbed increases linearly with

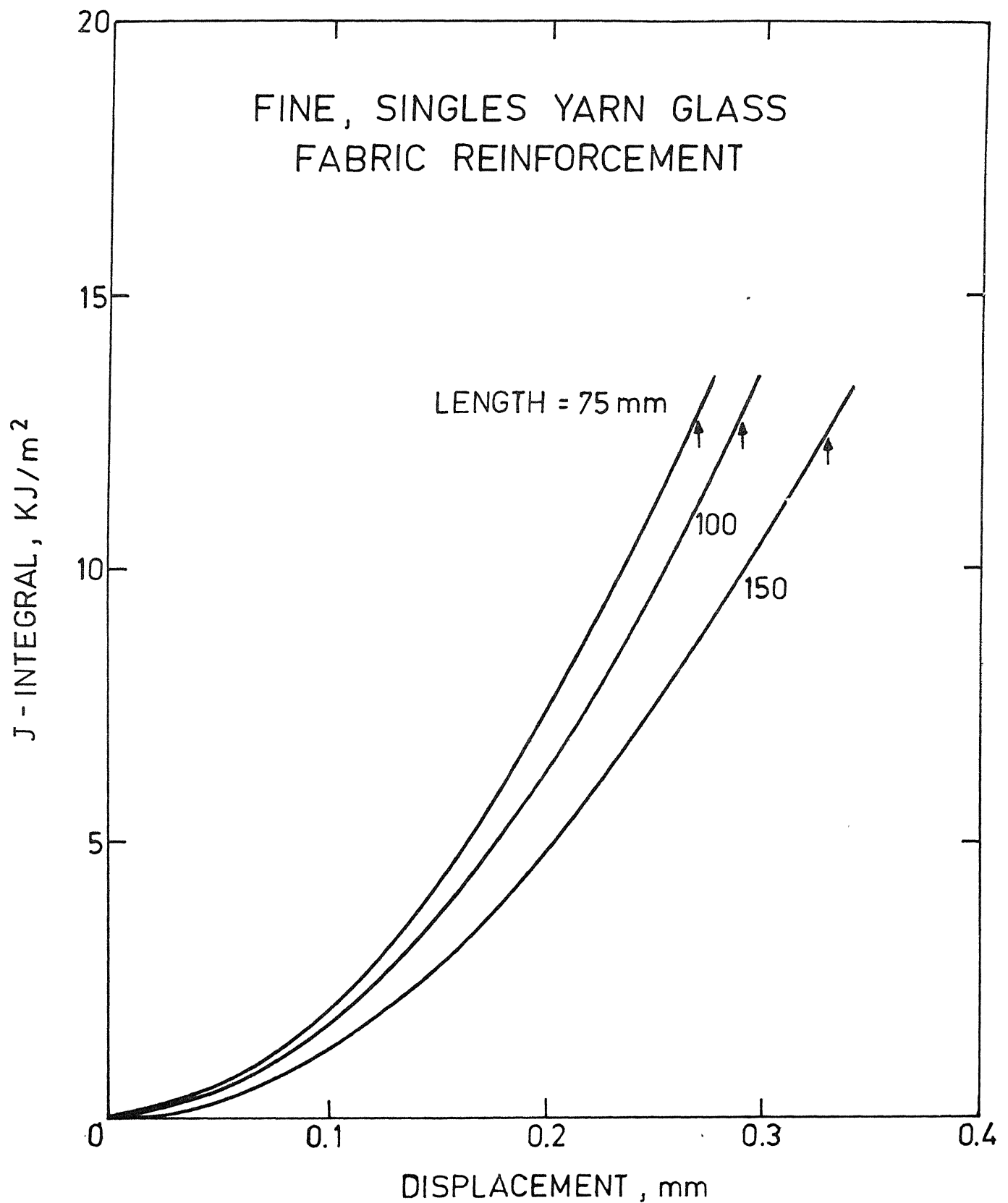


FIG. 3.20 J-INTEGRAL CURVES FOR SPECIMENS OF DIFFERENT LENGTHS FOR TYPE - A REINFORCEMENT.

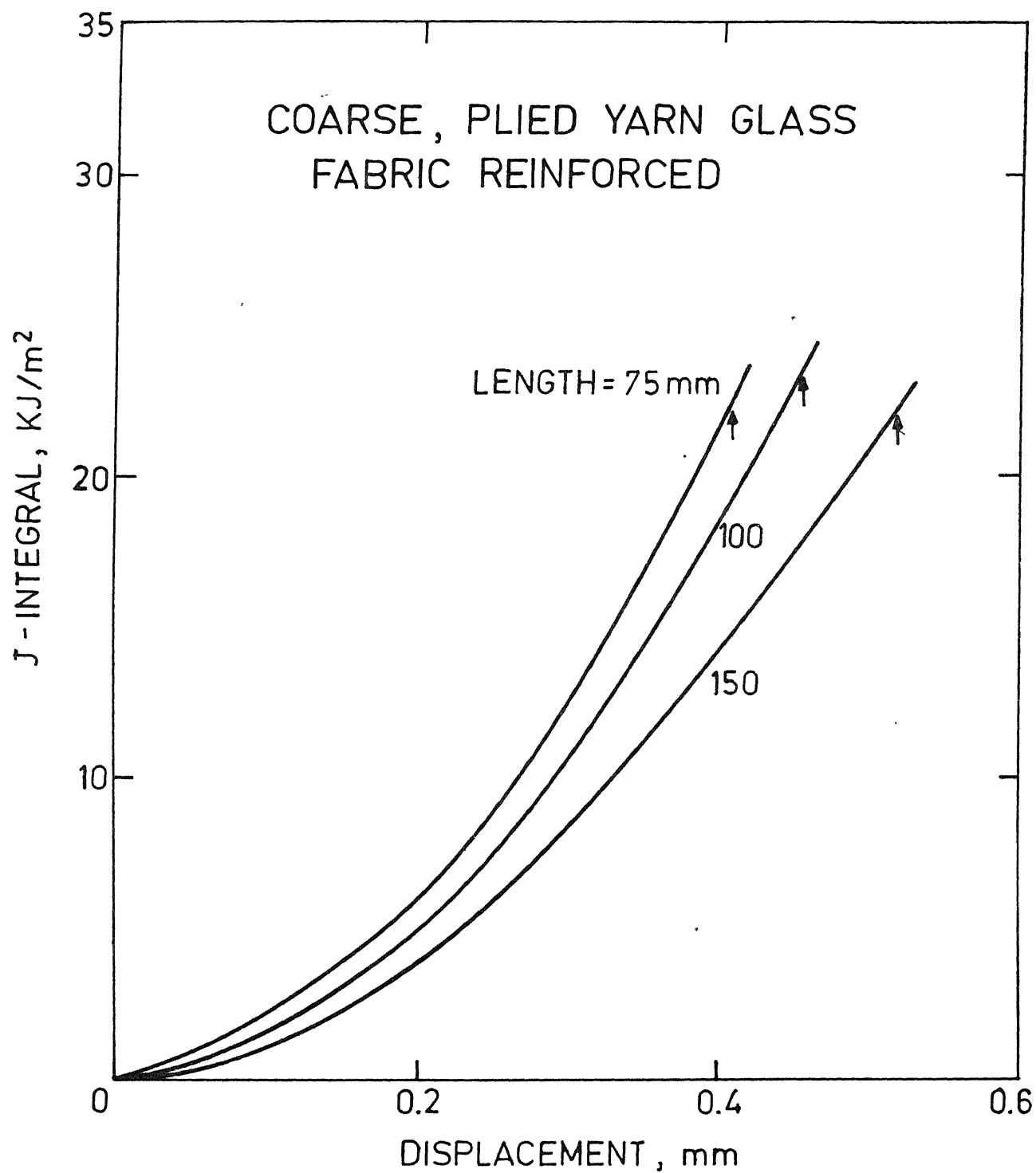


FIG. 3.21 J-INTEGRAL CURVES FOR SPECIMENS OF DIFFERENT LENGTHS FOR TYPE-B REINFORCEMENT.

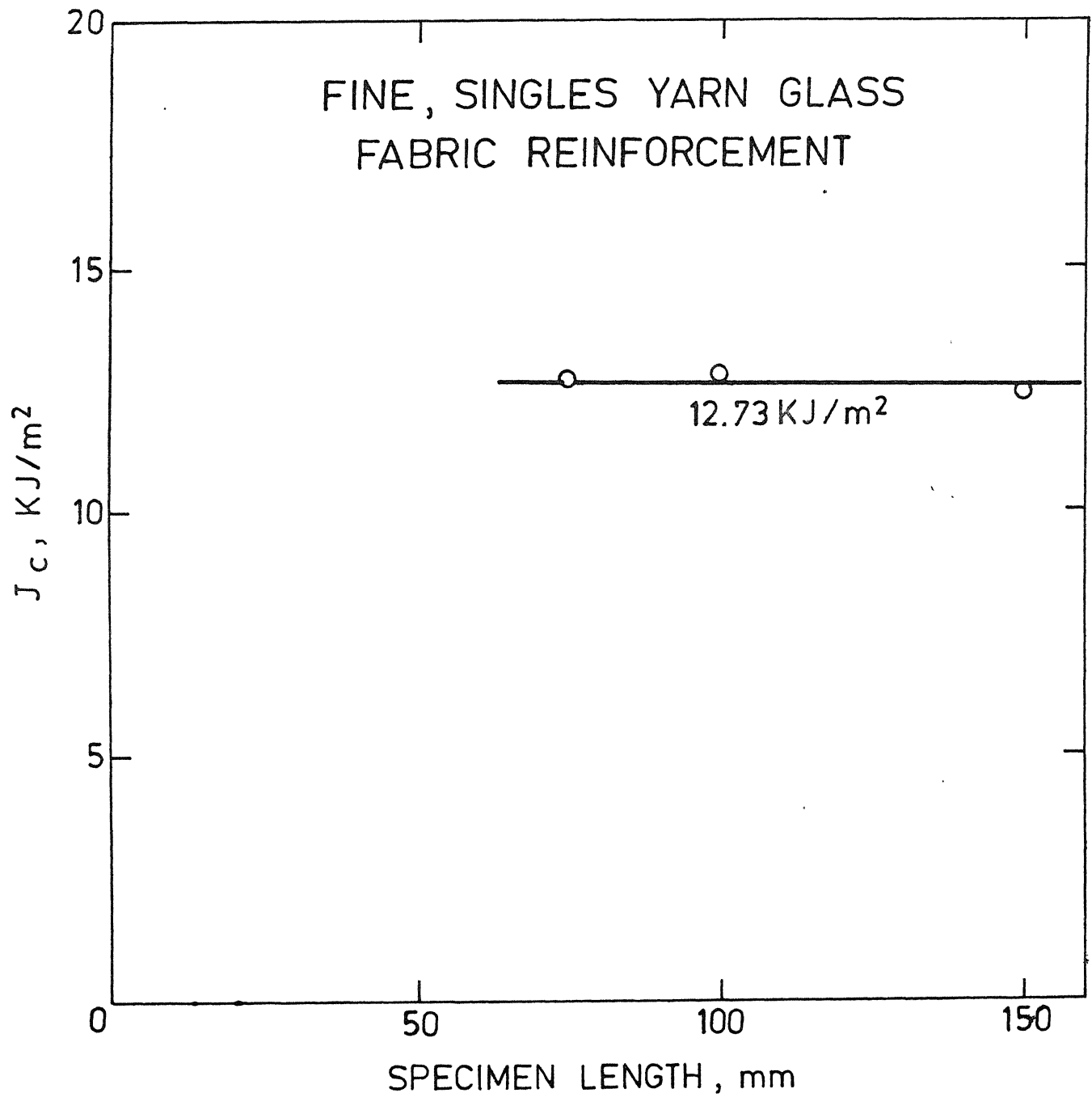


FIG. 3.22 INFLUENCE OF SPECIMEN LENGTH ON J_c FOR TYPE-A REINFORCEMENT.

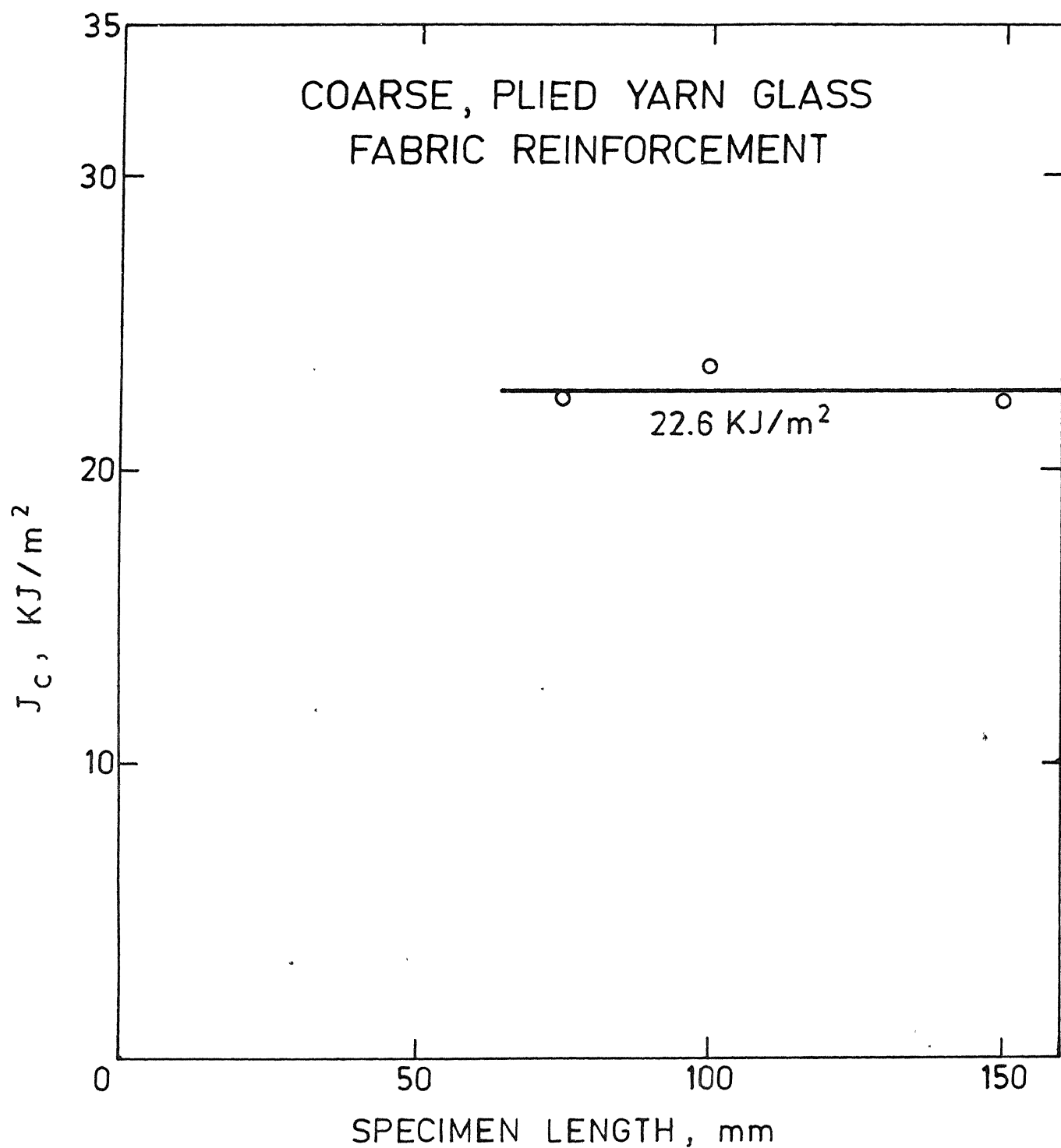


FIG. 3.23 INFLUENCE OF SPECIMEN LENGTH ON J_c FOR TYPE-B REINFORCEMENT.

specimen length, indicating a significant energy absorption in the region away from the crack tip as well.

These observations are further supported by visual observations of the specimens. The damage in the specimens with cracks larger than 12.5 mm is confined to the crack tip region, whereas in specimens with smaller cracks the damage is all over. This is illustrated in Fig. 3.24 through a photograph of two fractured specimens. The photograph was taken in bright light background and so the damage is indicated by dark areas.

The intercept on the ordinate obtained by extrapolation of a straight line in fig. 3.18 may be regarded as the energy absorbed in the crack tip region. This energy absorbed is plotted against crack length in Fig. 3.25. It has already been explained with respect to fig. 3.16 that the critical displacement due to the presence of a crack alone is independent of crack length. Thus it may be argued that the energy absorbed for different crack lengths (Fig. 3.25) corresponds to the same critical displacement and therefore, the slope of the straight line may be used to obtain the critical value of J , independent of the crack length. The J critical, J_{1C} , thus obtained is 13.8 KJ/m^2 which is close to the value of 12.7 KJ/m^2 obtained earlier in fig. 3.22. This shows that the energy absorbed at the

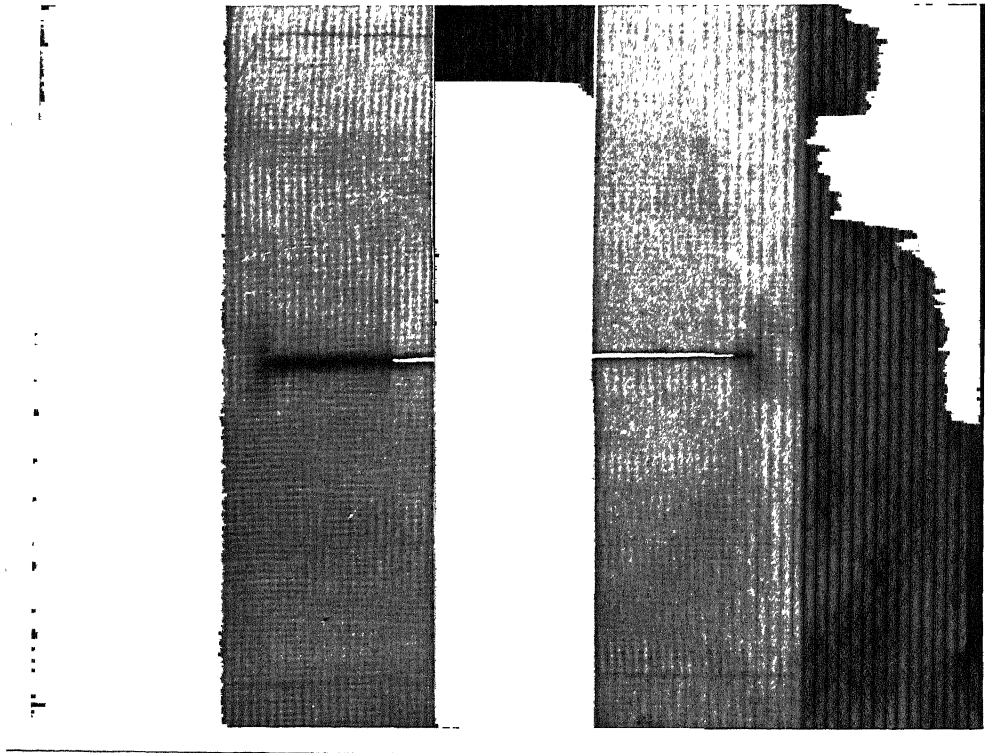


FIG. 3.24 : TRANSMITTED LIGHT PHOTOGRAPH OF
TWO SPECIMENS WITH TYPE-A
REINFORCEMENT, FOR DIFFERENT
CRACK LENGTHS.

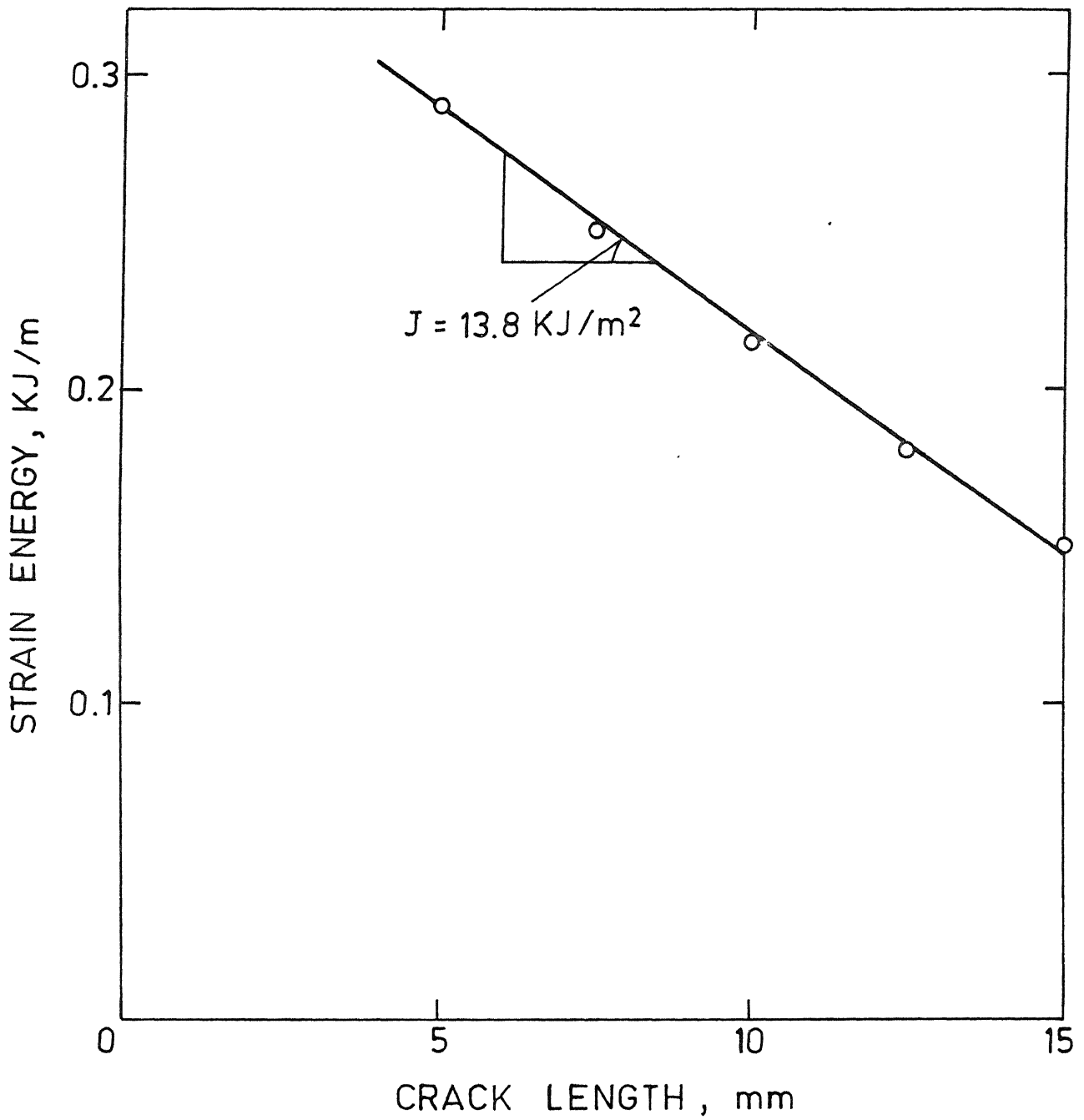


FIG. 3.25 STRAIN ENERGY AT CRACK TIP FOR DIFFERENT CRACK LENGTHS.

crack tip region may be separated from the energy absorbed in the region away from it. Thus, a parameter independent of testing variables - crack length and specimen length, is obtained. This value of J_{1C} may be used as a fracture criterion for glass fabric reinforced epoxy resin.

3.1.3 EFFECT OF SPECIMEN WIDTH:

The effect of specimen width on the fracture toughness (J_{1C}) of the glass fabric reinforced epoxy resin laminates with type A reinforcement was studied by varying specimen width from 15 mm through 25 mm, 35 mm, to 40 mm. The thickness in all cases was 2 mm and fibre volume fraction 39.5%. The length of specimens between grips was at least three times the width. For each width and crack length at least three samples were tested. Specimens with crack size $a_0/w \geq 0.4$ were tested.

The load displacement curves for specimens with different widths are shown in Figs. 3.26 to 3.29. The critical displacement is plotted against a_0/w in Fig. 3.30. It remains constant for a_0/w larger than 0.5. This constant value however depends on the specimen width; it increases with specimen width.

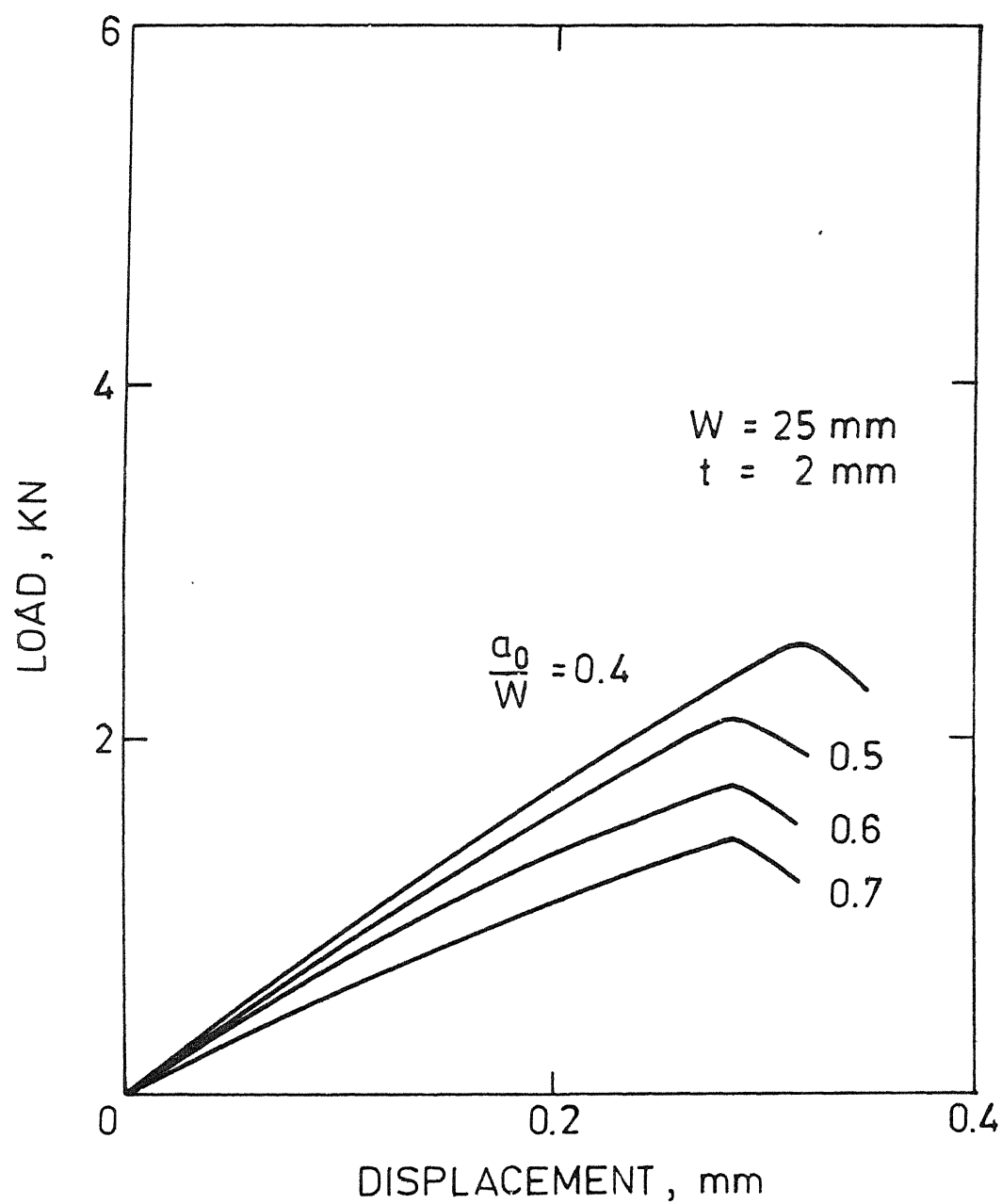


FIG. 3.26 LOAD DISPLACEMENT CURVES FOR 15 mm WIDE SPECIMENS.

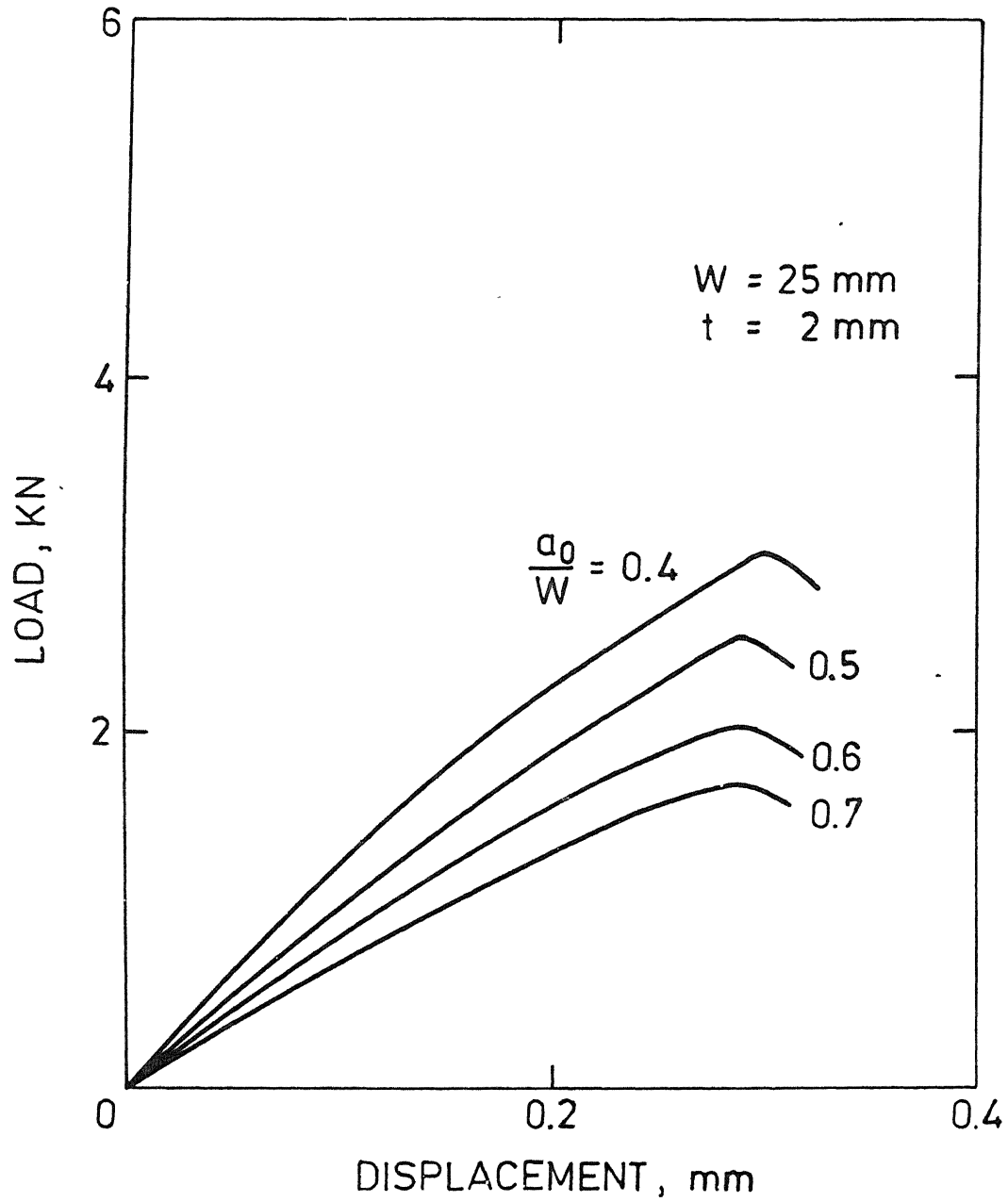


FIG. 3.27 LOAD DISPLACEMENT CURVES FOR 25 mm WIDE SPECIMENS.

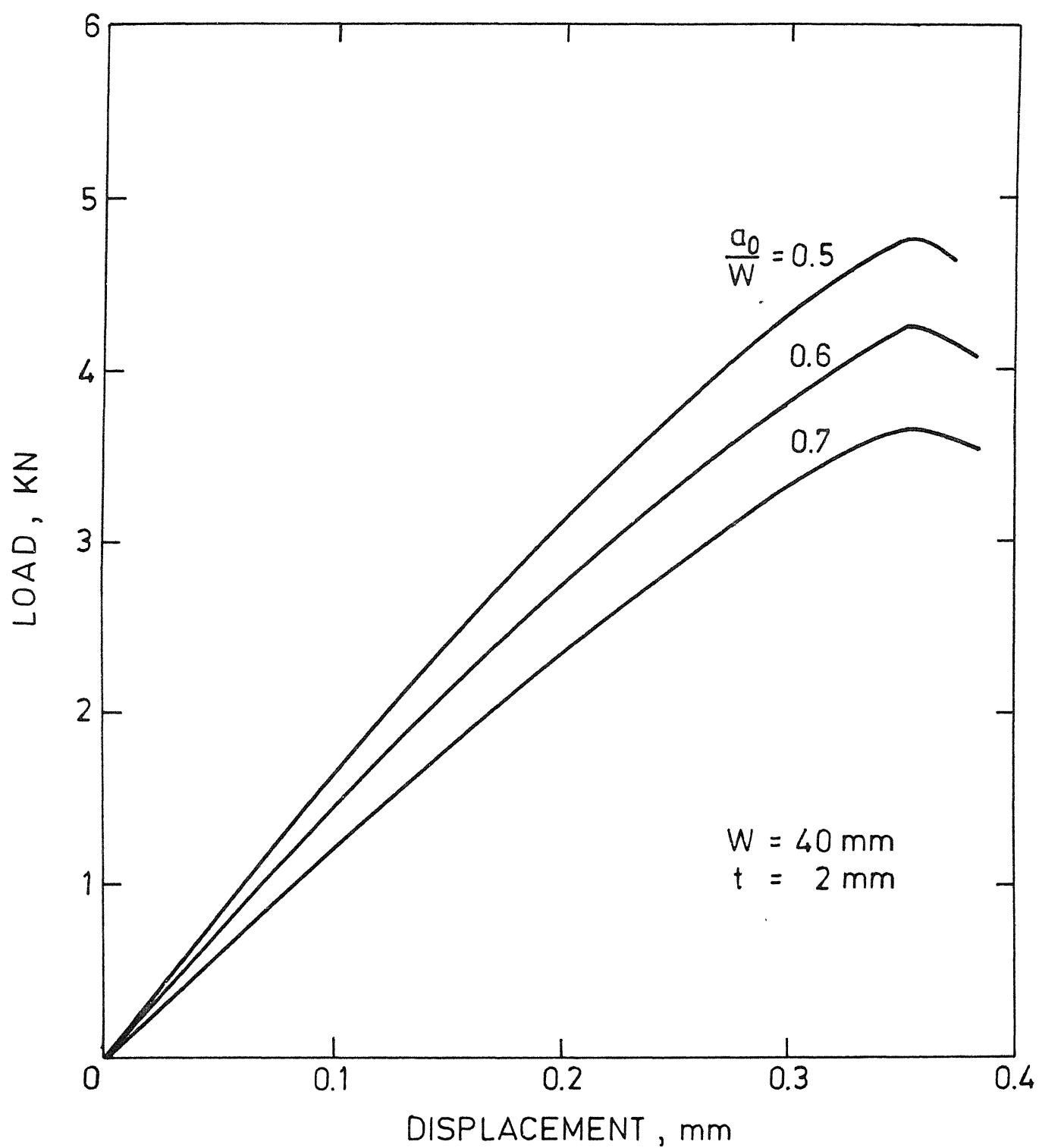


FIG. 3.29 LOAD DISPLACEMENT CURVES FOR 40 mm WIDE SPECIMENS.

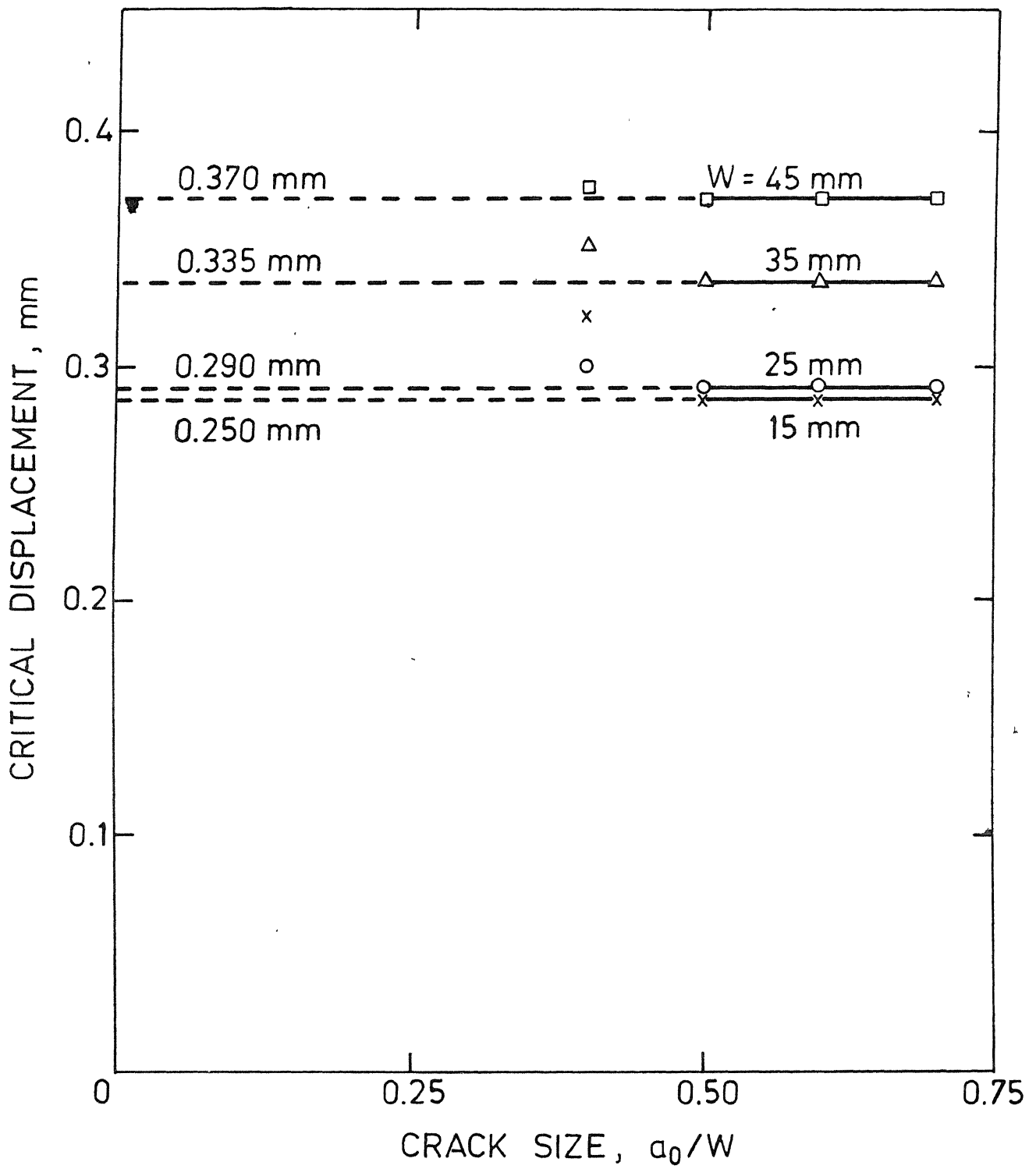


FIG. 3.30 EFFECT OF SPECIMEN WIDTH ON CRITICAL DISPLACEMENTS.

The J-integral for each width is obtained as a function of displacement using its energy rate interpretation. The J curves for different specimen widths are shown in Fig. 3.31. Corresponding to the constant critical displacements obtained earlier (Fig. 3.30), the critical value of J-integral, J_{1C} , is obtained for each width in fig. 3.31. These values of J_{1C} plotted against specimen width in Fig. 3.32 do not exhibit any trend with specimen width. The small variation is random. Thus, J_{1C} may be taken to be independent of specimen width. An average value of J_{1C} is 13.7 KJ/m^2 . This value is close to the value of 12.7 KJ/m^2 obtained earlier in sec. 3.1.2.

3.1.4 EFFECT OF STYLE OF REINFORCEMENT ON MECHANICAL PROPERTIES AND FRACTURE TOUGHNESS:

The mechanical properties of the laminates with two different styles of reinforcement are given in table 3.1. The laminates with type-A reinforcement, (Fine, plain weave, balanced, untwisted yarn glass fabric), show higher modulus of elasticity, ultimate tensile strength and shear modulus compared to laminates with type-B reinforcement, (coarse, plain weave, balanced, twisted yarn glass fabric).

The higher modulus of elasticity and ultimate tensile strength of type-A laminates is due to the

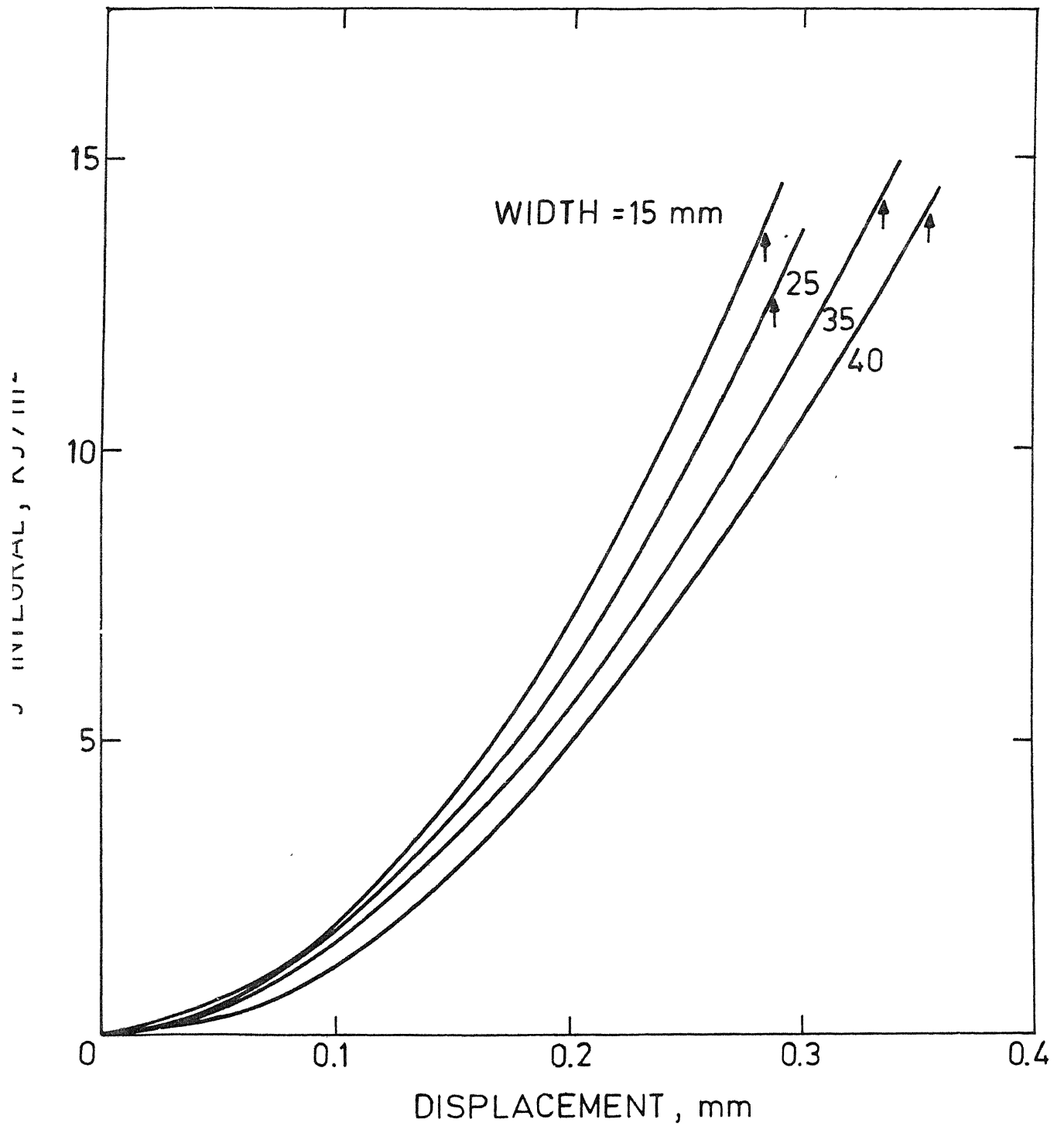


FIG. 3.31 J-INTEGRAL CURVES FOR SPECIMENS OF DIFF. ERENT WIDTH.

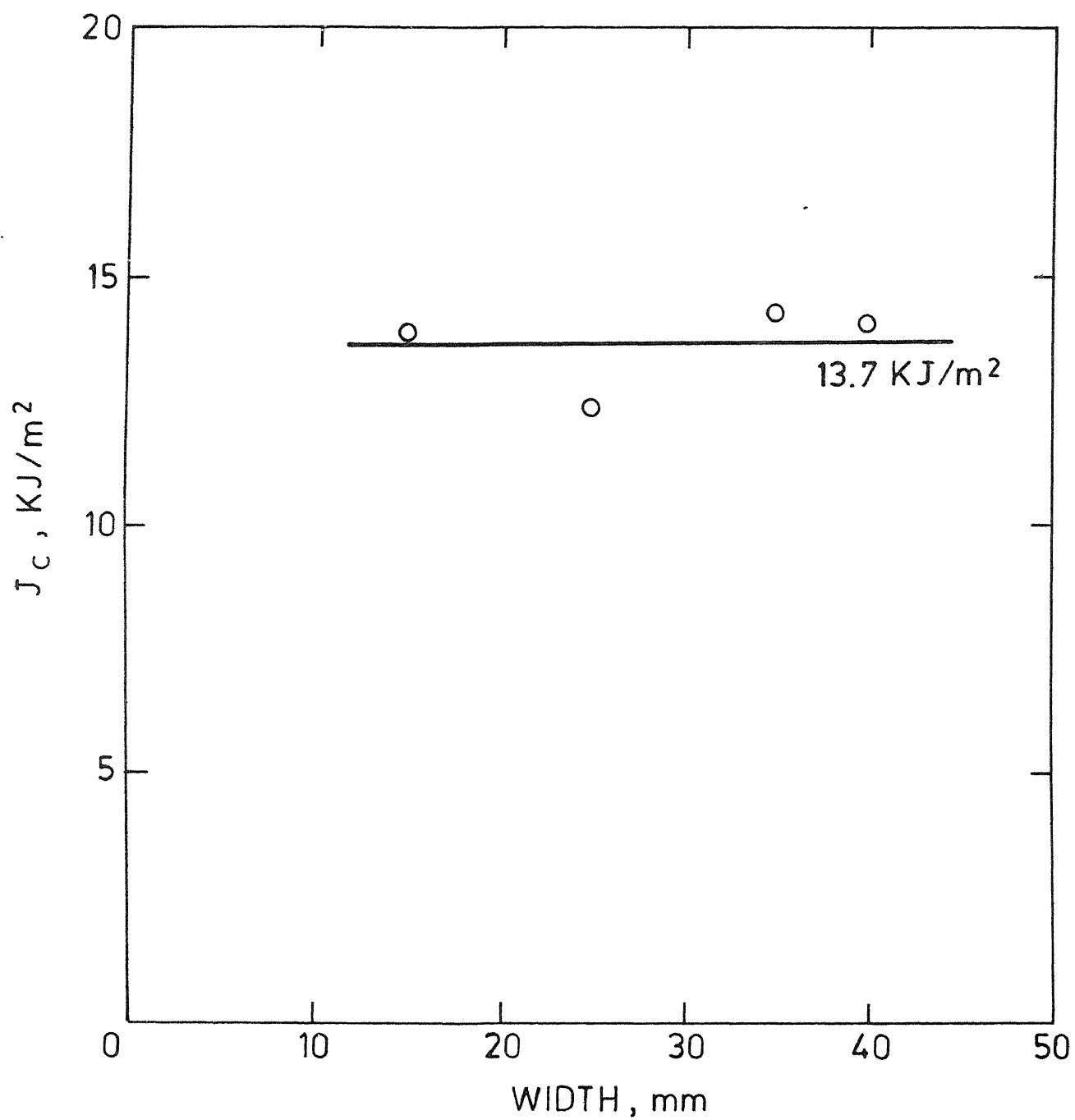


FIG. 3.32 INFLUENCE OF WIDTH ON J_c .

parallel alignment of filaments in singles-yarn fabric, which exposes more surface area for glass-to-resin binding. Thus in type-A laminates the glass fabric is very well impregnated by the resin. In type-B laminates the glass fabric being of the plied yarn type is difficult to impregnate with resin. In fact, it was observed on a close visual inspection that the resin had only partially impregnated the glass fabric. Due to the above two reasons type-B laminates show a much lower modulus of elasticity. However, the ultimate tensile strength is only slightly lower for type-B laminates compared to type-A laminates. This is due to the larger crimp at yarn cross over in type-B reinforcement as compared to type-A reinforcement.

Laminates with type-B reinforcement exhibit a much higher fracture toughness compared to type-A reinforced laminates for nearly the same volume fraction. This may be due to the improper impregnation of resin. Also a low value of shear modulus for type-B laminates permits greater shear deformation.

3.2 EVALUATION OF J_{1C} FOR $\pm 45^\circ$ LAMINATES:

Fracture toughness studies have been performed on $\pm 45^\circ$ glass cloth reinforced epoxy resin laminates, to study the effect of fiber orientation on fracture

toughness. The type A glass cloth reinforcement (sec. 2.1) was used. Specimens 25 mm wide, 100 mm long and crack lengths varying between 0.1 and 0.7 of specimen width were tested in displacement control mode.

Typical load displacement curves with different initial crack lengths are shown in Fig. 3.33. Specimens with small cracks fracture suddenly causing an abrupt drop in load, whereas specimens with larger cracks show a more gradual fracture behaviour. The critical displacement is plotted against crack length in Fig. 3.34. For small crack lengths the critical displacement decreases with increase in a_0 but remains constant for crack size $a_0/w \geq 0.5$ or 12.5 mm. This behaviour is similar to that seen for $0^\circ/90^\circ$ glass cloth reinforced epoxy laminates earlier in sec. 3.1.1. The value of this constant critical displacement is 0.27 mm. For $0^\circ/90^\circ$ laminates of same thickness and volume fraction the constant critical displacement is 0.29 mm. Thus the critical displacement for crack lengths of $a_0/w > 0.5$ does not depend on fiber orientation in glass cloth reinforced epoxy laminates. The critical displacement depends on the effective resistance offered by reinforcement to the deformation of the matrix. This resistance possibly does not change with orientation for glass cloth reinforced epoxy composites. The strain

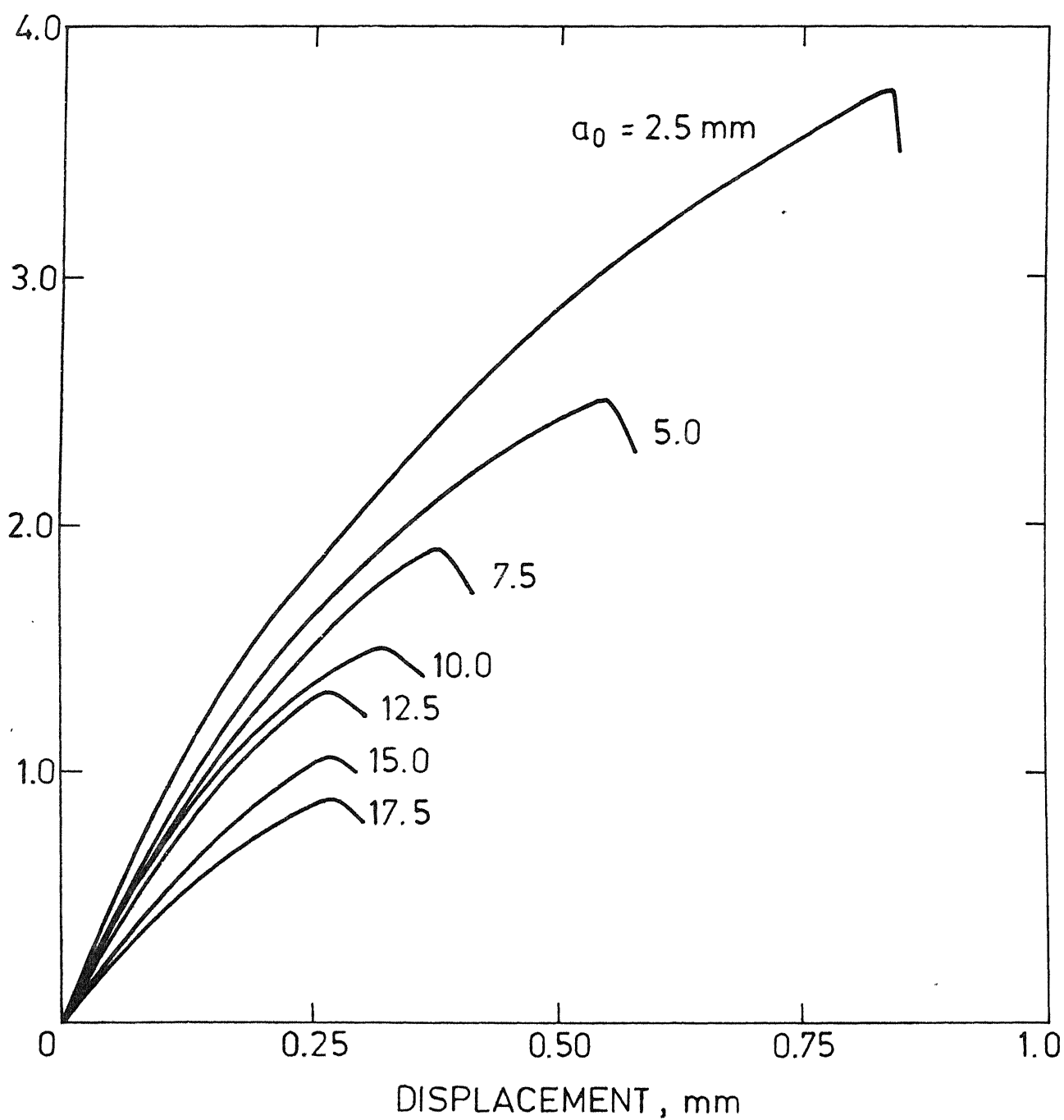


FIG. 3.33 LOAD DISPLACEMENT CURVES FOR $\pm 45^\circ$ ANGLE PLY SPECIMENS.

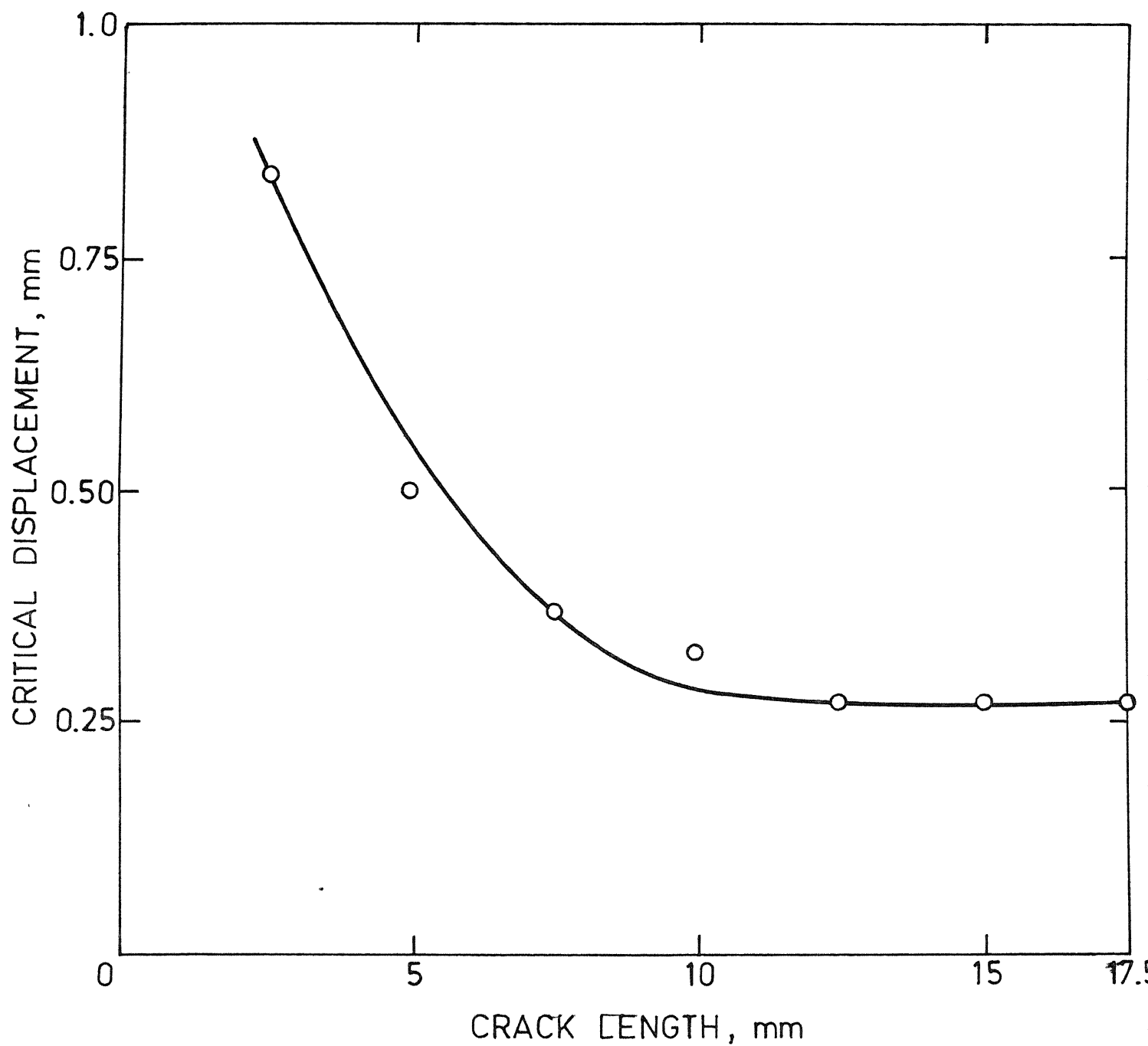


FIG. 3.34 VARIATION OF CRITICAL DISPLACEMENT WITH CRACK LENGTH FOR $\pm 45^\circ$ ANGLE PLY SPECIMEN.

energy per unit thickness for different displacements is plotted as a function of crack length in Fig. 3.35. These energy curves are similar to that obtained for $0^\circ/90^\circ$ laminates. For the same reasons as discussed in sec. 3.1.1. The J-integral is calculated corresponding to different displacement for cracks longer than 12.5 mm or $a_0/w > 0.5$. The variation of J with displacement is shown in Fig. 3.36. The critical value of J, J_{1C} , corresponding to the constant value of critical displacement, is obtained to be 5.74 KJ/m^2 . For crack lengths less than $a_0/w = 0.5$, J_{1C} cannot be uniquely determined due to the general material damage away from the crack tip (Fig. 3.24) as well (sec. 3.1.1 and sec. 3.1.2).

Thus as can be expected, the value of J_{1C} depends strongly on the fiber orientation. The value of J_{1C} for $\pm 45^\circ$ laminates is less than half of that for $0^\circ/90^\circ$ laminates. So the $\pm 45^\circ$ glass cloth reinforced angle ply laminates cannot be used for structural applications due to their low fracture toughness.

3.3 CONCLUSIONS:

The fracture behaviour of glass fabric reinforced epoxy composites has been investigated. The J-integral has been evaluated using the energy rate

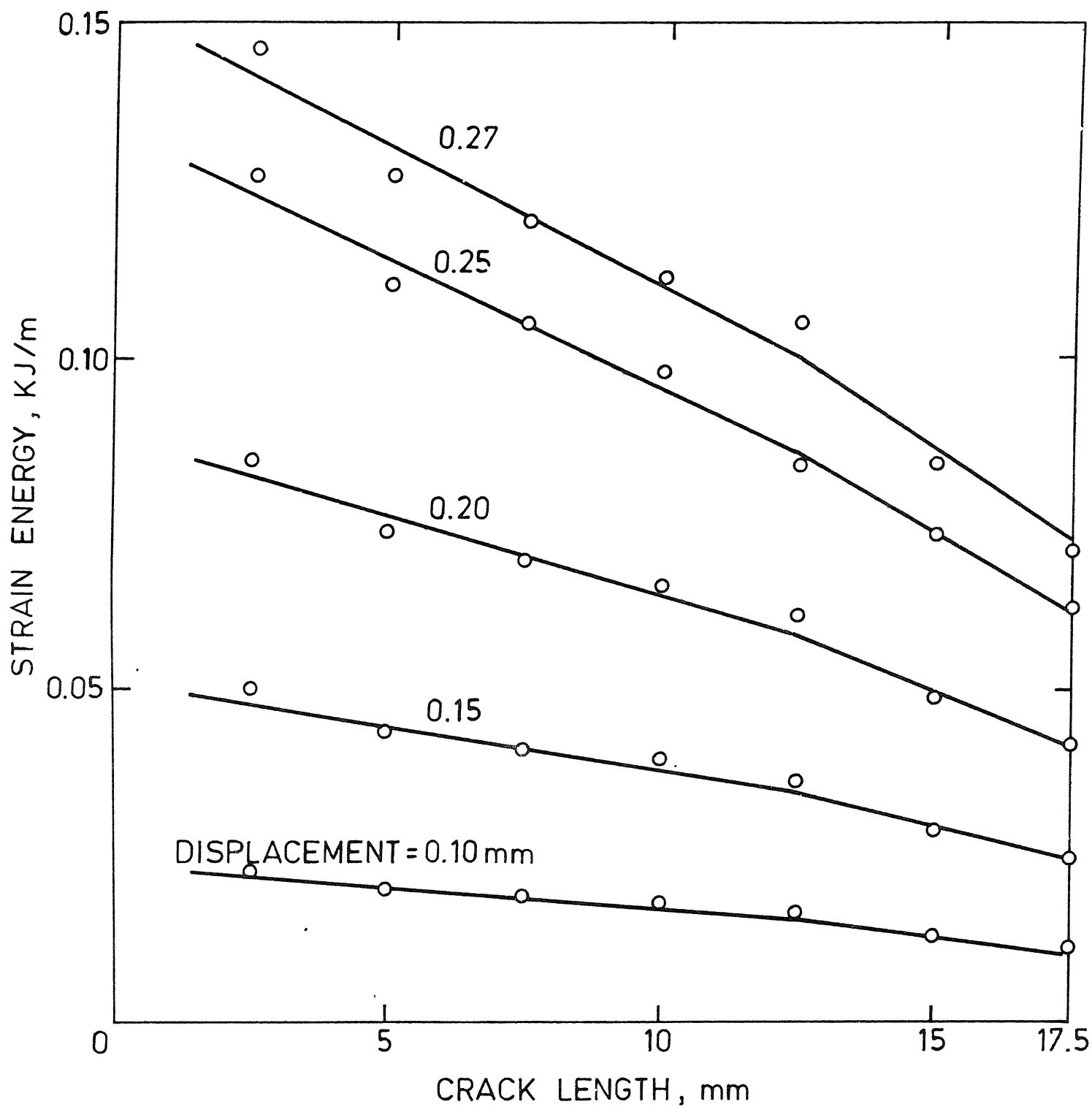


FIG. 3.35 STRAIN ENERGY PER UNIT THICKNESS FOR DIFFERENT DISPLACEMENTS FOR $\pm 45^\circ$ ANGLE PLY SPECIMENS.

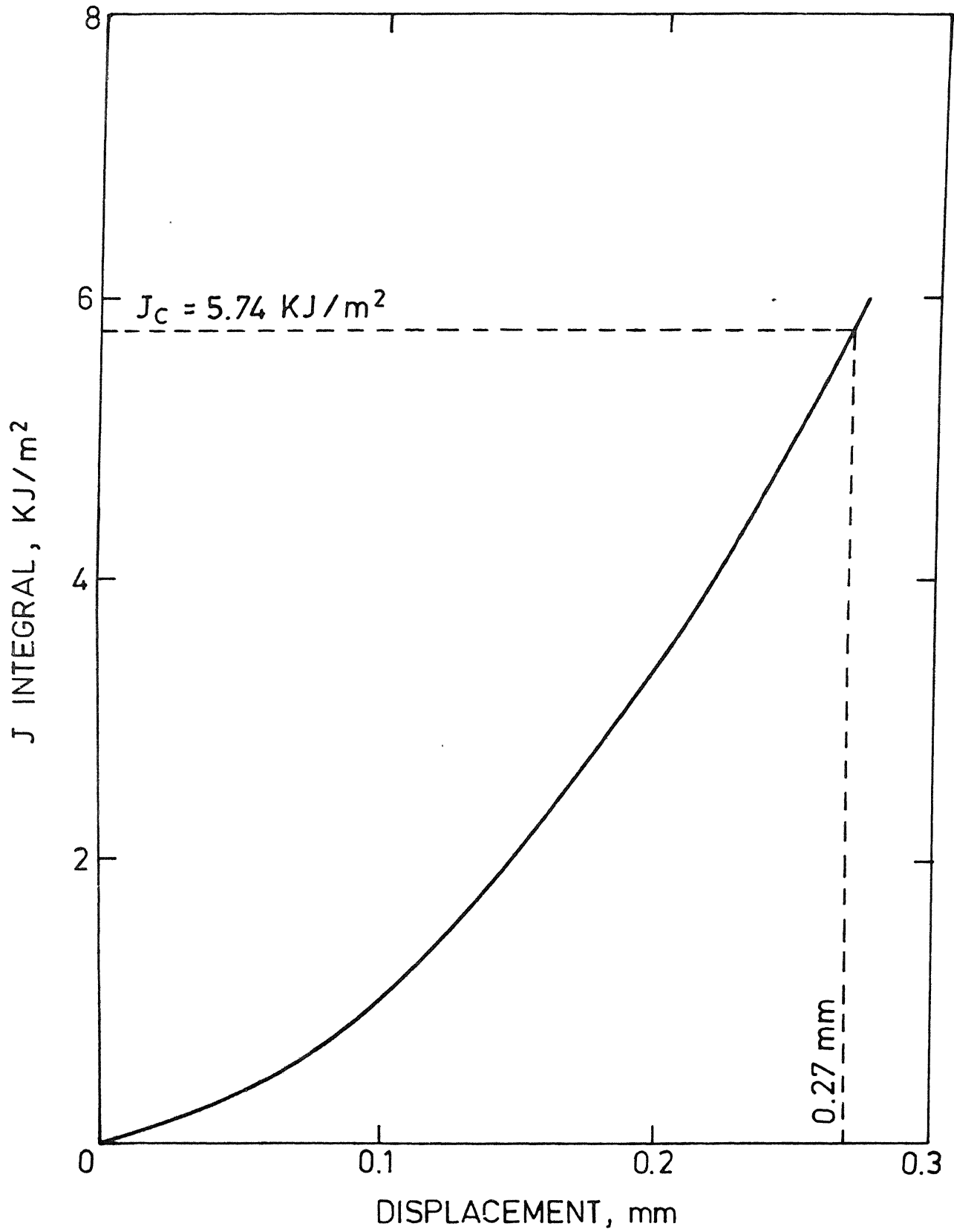


FIG. 3.36 J-INTEGRAL CURVE FOR $\pm 45^\circ$ ANGLE PLY SPECIMENS.

interpretation. Its value is found to be independent of crack length when the ratio of crack length to specimen width (a_0/w) is larger than 0.5. For smaller crack lengths the general material damage away from the crack tip also influences the energy absorbed significantly. However, an extrapolation method has been used through which the crack tip energy may be separated from the energy absorbed due to general material damage. The J-integral thus obtained is independent of crack length and specimen length and its critical value is the same as obtained for $a_0/w > 0.5$ without extrapolation.

Two types of laminates - type A with fine, plain weave, balanced, untwisted yarn glass fabric reinforcement and type B with coarse, plain weave, balanced, twisted yarn glass fabric reinforcement - were tested. The fracture behaviour of both the laminates is similar. However, the type A laminates possess a higher strength but much lower fracture toughness compared to type B laminates. J_{1C} for type A laminates is 12.8 KJ/m^2 and for type B it is 22.6 KJ/m^2 . It seems that the type of twist and plying of glass fibers significantly affects the fracture toughness.

The critical value of J-integral, J_{1C} , is found to be independent of width of specimen for $a_0/w > 0.5$.

J_{1C} is found to depend strongly on fiber orientation. For $\pm 45^\circ$ laminates, J_{1C} is found to be 5.76 KJ/m^2 which is very low compared to 12.8 KJ/m^2 for $0^\circ/90^\circ$ laminates.

3.4 SCOPE FOR FURTHER WORK:

- (1) Other varieties of glass cloth reinforcement should be employed to find the most effective reinforcement and find the effect of cloth variables like fiber diameter, strand diameter, twist and plying of fibers, on fracture toughness.
- (2) Find how fracture toughness varies with cloth orientation. Thus experiments should be carried out for fiber orientations of 15° and 30° also.

REFERENCES

- [1] A.A. Griffith, "The Phenomena of Rupture and Flow in Solids", Phil. Trans. Roy. Soc. of London, A 221, 1920, pp 163-197.
- [2] G.R. Irwin, "Analysis of Stresses and Strains Near the End of a Crack Traversing a Plate", Trans. ASME, J. Applied Mechanics, Vol. 24, 1957, pp 361-364.
- [3] M.J. Owen and P.T. Bishop, "Critical Stress Intensity Factors Applied to Glass Reinforced Polyster Resin", J. Composite Materials, Vol.7, 1973, pp 146-159.
- [4] J.F. Madell, S.S. Wang and F.J. McGarry, "The Extension of Crack Tip Damage Zones in Fiber Reinforced Plastic Laminates", J. Composite Materials, Vol. 9, 1975, p 266.
- [5] J.M. Slepetz and L. Carlsen, "Fracture of Composite Compact Tension Specimens", Fracture Mechanics of Composites, ASTM STP 593, American Society for Testing and Materials, 1974, pp 143-162.
- [6] S.Guofang, "Fracture of Fiberglass Reinforced Composites", J. Composite. Materials, Vol. 15, 1981, pp 521-530.
- [7] R.J. Lee and D.C. Phillips, "Fracture Toughness Testing of High Performance Laminates", Conference on Testing Evaluation and Quality Control of Composites, held at Guildford, September, 1983.

- [8] S.K. Gagger and L.J. Broutman, " Crack Growth Resistance of Random Fiber Composites", J. Composite Materials, Vol. 9, 1975, pp 216-227.
- [9] S.K. Gagger and L.J. Broutman, " Effect of Crack Tip Damage on Fracture of Random Fiber Composites", Materials Science and Engineering, Vol. 21, 1975, pp 177-183.
- [10] B.D. Agarwal and G.S. Giare, " Crack Growth Resistance of Short Fiber Composites: I - Influence of Fiber Concentration, Specimen Thickness and Width", Fiber Science and Technology, Vol. 15, 1981, pp 283-298.
- [11] D.H. Morris and H.T. Hahn, " Fracture Resistance Characterization of Graphite/Epoxy Composites", Composite Materials Testing and Design (Fourth Conference) ASTM STP 617, American Society for Testing and Materials, Philadelphia, 1977, pp 5-17.
- [12] J.R. Rice, " A Path Independent Integral and the Approximate Analysis of Strain Concentration by Notches and Cracks", J. Applied Mechanics, Vol. 35, 1968, pp 379-386.
- [13] K.B. Broberg, " Crack Growth Criteria and Non-linear Fracture Mechanics", J. Mechanics and Physics of Solids, Vol. 19, 1971, pp 407-418.
- [14] J.W. Hutchinson, " Singular Behaviour at the End of a Tensile Crack in a Hardening Material", J. Mechanics and Physics of Solids, Vol. 16, 1968, pp 13-31.

- [15] J.R. Rice and G.F. Rosengren, "Plane-strain Deformation Near a Crack Tip in a Power Law Hardening Material", J. Mechanics and Physics of Solids, Vol. 16, 1968, pp 1-12.
- [16] F. McClintock, "Plasticity Aspects of Fracture", Chapter 2, Fracture, Vol. III, Ed. H. Liebowitz, Academic Press, New York, 1971, pp 47-225.
- [17] J.A. Begley and J.D. Landes, "The J-integral as a Fracture Criterion", Fracture Toughness, ASTM STP 514, American Society for Testing and Materials, Philadelphia, 1972, pp 1-20.
- [18] B.D. Agarwal, B.S. Patro, Prashant Kumar, "J-integral as a Fracture Criterion for Short Fiber Composites : An Experimental Approach", Engineering Fracture Mechanics, Vol. 19, No. 4, 1984, pp 675-684.
- [19] K. Srinivasan, "Fracture Toughness of Quasi-Isotropic and Cross-plyed Laminates using J-integral Approach", M. Tech. Thesis, Indian Institute of Technology, Kanpur, India, May, 1984.
- [20] G. Smith, A.K. Green and W.H. Bowyer, "The Fracture Toughness of Glass Fabric Reinforced Polyester Resins", Fracture Mechanics in Engineering Practice, Ed. P. Stanley, Applied Science Publishers, 1977, pp 271-287.

A 6103

ME-1984-m-KHA-FRA